

DOKUZ EYLÜL UNIVERSITY
GRADUATE SCHOOL OF NATURAL AND APPLIED SCIENCES

**AUTO-MEASUREMENT FOR STENT GRAFT &
VIRTUAL POST STENT ENDOVASCULAR
EVALUATION OF EVAR**

by
Hulusi BAYSAL

May, 2011
İZMİR

**AUTO-MEASUREMENT FOR STENT GRAFT &
VIRTUAL POST STENT ENDOVASCULAR
EVALUATION OF EVAR**

**A Thesis Submitted to the
Graduate School of Natural and Applied Sciences of Dokuz Eylül University
In Partial Fulfillment of the Requirements for the Degree of Doctor Philosophy in
Computer Engineering, Computer Engineering Program**

**by
Hulusi BAYSAL**

**May, 2011
İZMİR**

PhD. THESIS EXAMINATION RESULT FORM

We have read the thesis entitled “**AUTO-MEASUREMENT FOR STENT GRAFT & VIRTUAL POST STENT ENDOVASCULAR EVALUATION OF EVAR**” completed by **HULUSI BAYSAL** under supervision of **PROFESSOR DR. ALP KUT** and we certify that in our opinion it is fully adequate, in scope and in quality, as a thesis for the degree of Doctor Philosophy.



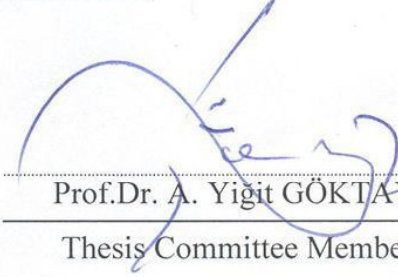
Prof.Dr. Alp KUT

Supervisor



Prof.Dr. Yalçın ÇEBİ

Thesis Committee Member



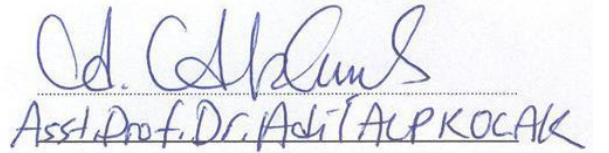
Prof.Dr. A. Yigit GÖKTAY

Thesis Committee Member



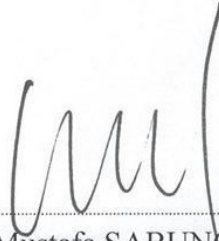
Doc. Dr. Onur Demirel

Examining Committee Member



Asst. Prof. Dr. Adil ALPKOÇAK

Examining Committee Member



Prof.Dr. Mustafa SABUNCU

Director

Graduate School of Natural and Applied Sciences

ACKNOWLEDGEMENTS

I would like to express my gratitude to my supervisor, Prof. Dr. Alp KUT, whose expertise, understanding, and patience, added considerably to my graduate experience.

I extend my thanks to the members of my committee, Prof. Dr. Yalçın ÇEBİ, and Asst. Prof. Dr. Yiğit GÖKTAY for their useful comments and suggestions during my study.

I thank my family, all my friends and professors for their support during my study. Especially Semih UTKU, Tolga BERBER and Ömür GENCEL.

In addition, I would like to acknowledge the support from the Dokuz Eylül University BAP for the equipment support for this thesis.

Hulusi BAYSAL

AUTO-MEASUREMENT FOR STENT GRAFT & VIRTUAL POST STENT ENDOVASCULAR EVALUATION OF EVAR

ABSTRACT

The use of computer systems has influenced every area of the society including medical. In medical diagnosis, it is highly desirable to have detailed information on the anatomical and pathological features of the patient as possible. Medical visualization can help to overcome this problem by providing a 3D representation of the patient's anatomy.

This thesis introduces a medical visualization platform and measurement methods to help physicians in determining appropriate stent grafts for abdominal aortic aneurysms and diagnosing the aneurysm before and after stent graft repair. Selection of an appropriate stent graft for the aneurysm requires accurate measurements of the aorta and the aneurysm. Platform provides various measurement capabilities on a generated 3D model of the aorta.

In this study, a system is proposed which generates 3D model of the aneurysm from computer tomography images using common segmentation and modeling methods. System provides measurement methods to gather crucial measurements such as aortic neck angulations and aneurysm length before EVAR operation for appropriate stent selection.

Several evaluation methods were performed on the data models to verify the accuracy of the system. The results showed that the system has a high reliability.

Keywords: Abdominal Aortic Aneurysm, Medical Applications, 3D Modeling, Medical Imaging, EVAR, Stents.

STENT İÇİN OTOMATİK ÖLÇÜMLEME VE SANAL DAMARIÇİ STENT UYGULAMASI SONRASI DEĞERLENDİRME

ÖZ

Bilgisayar sistemlerinin kullanımı, hayatın her alanını etkilediği gibi sağlık alanını da etkilemiştir. Tıbbi teşhiste hastanın anatomic ve patolojik özellikleri hakkında detaylı bilgi edinmek önem arz etmektedir. Tıbbi görüntüleme hastanın anatomisini üç boyutlu olarak sunarak bu sorunun üstesinden gelinmesine yardımcı olmaktadır.

Bu tez, abdominal aort anevrizması için uygun stent belirlenmesi ve anevrizmanın stent tedavisi öncesi ve sonrası durumunun incelenmesi için uzmanlara yardımcı olacak tıbbi görüntüleme platformu ve ölçüm metodları sunmaktadır. Anevrizmaya uygun stent seçimi aort ve anevrizmaya ait ölçümlerin doğru olarak alınmasına bağlıdır. Uygulama platformu, oluşturulmuş üç boyutlu model üzerinde çeşitli ölçüm yöntemleri sunmaktadır.

Bu çalışmada, yaygın bölütleme ve modelleme yöntemleri ile bilgisayarlı tomografi resimlerinden üç boyutlu anevrizma modelini oluşturmak için bir sistem sunulmaktadır. Çalışma, EVAR operasyonu için uygun stent seçimi ve operasyon sonrası hastanın takibi için gerekli aort boyun açısı ve anevrizma uzunluğu gibi kritik ölçümlerin güvenilir biçimde elde edilmesinde katkı sağlamaktadır.

Sistemin tutarlılığını test etmek için veri modelleri üzerinde çeşitli değerlendirme metodları uygulanmıştır. Sonuçlar sistemin yüksek bir güvenilirliğe sahip olduğunu göstermiştir.

Anahtar Kelimeler: Abdominal Aort Anevrizması, Sağlık Uygulamaları, 3B modelleme, medikal görüntüleme, EVAR, Stentler

CONTENTS

THESIS EXAMINATION RESULT FORM	Error! Bookmark not defined.
ACKNOWLEDGEMENTS	iii
ABSTRACT	iv
ÖZ	v
CHAPTER ONE - INTRODUCTION.....	1
1.1 Background and Problem Definition	2
1.2 Contributions of Thesis	3
1.3 Thesis Organization	5
CHAPTER TWO - ABDOMINAL AORTIC ANEURYSMS	7
2.1 Abdominal Aortic Aneurysms	7
2.2 Diagnosis of Aneurysm and Treatment Methods	9
2.2.1 Treatment Methods.....	10
2.2.2 Patient Selection	13
2.2.3 EVAR Parameters	15
2.3 Measurement Steps in Radio Diagnostic Department	17
CHAPTER THREE - RELATED WORKS	20
3.1 Related Works : Aortic Parameters.....	20
3.2 Related works: Aneurysm Diagnosis And Treatment Tools.....	21
3.2.1 Materialise Mimics	21
3.2.2 M2S Preview	22
3.2.3 TeraRecon Aquarius Intuition.....	23
3.2.4 3D Slicer	24
3.3 Deficiencies of Current Methods.....	24
CHAPTER FOUR - MEDICAL VISUALIZATION	26

4.1 Acquisition of Medical Images.....	27
4.1.1 Imaging Modalities.....	27
4.1.2 DICOM File Format.....	29
4.2 Image Processing.....	31
4.2.1 Segmentation.....	31
4.2.2 Clustering Methods.....	33
4.2.3 Histogram Based Methods.....	33
4.2.4 Edge Detection Methods.....	34
4.2.5 Region Growing Methods.....	34
4.3 Data Visualization.....	35
4.3.1 Marching Cubes Approach.....	36
4.3.2 Fair Tiling Approach.....	37
4.3.3 Comparison of Fair Tiling and Marching Cubes Methods.....	43
CHAPTER FIVE - ABDOMINAL AORTIC ANEURYSM MEASUREMENT AND EVALUATION TOOL	46
5.1 Abdominal Aortic Aneurysm Measurement And Evaluation Tool.....	46
5.1.1 Dicom Viewer.....	48
5.1.2 Aorta Segmentation.....	48
5.1.2.1 Extraction Of Aorta Boundary.....	52
5.1.2.2 Aortic Center Line Path.....	55
5.1.3 3D Visualization & Observation.....	58
5.1.4 Measurement and Evaluation.....	59
5.1.5 Stent Graft Selection.....	62
5.2 Web Based Aorta Visualization & Evaluation.....	64
5.2.1 Medical Data and Internet.....	65
5.2.2 3D Web Technologies.....	65
5.2.3 AortaWeb : An AMET extension.....	66
CHAPTER SIX - CASE STUDY	68
6.1 Patient Dataset.....	68
6.2 Measurement Methods.....	68
6.3 Measurement Evaluation.....	70

CHAPTER SEVEN - CONCLUSIONS.....	79
REFERENCES.....	82
APPENDICES.....	90
A. Measurement In Manual Method And AMET.....	90
B. Report Generation Module In AMET.....	94
C. Planes of The Body.....	99
D. ABBREVIATIONS.....	100

CHAPTER ONE

INTRODUCTION

The use of computer systems has influenced every area of the society including medical. There is a growing interest in the use of medical visualization tools. In medical diagnosis, it is highly desirable to have much detailed information on the anatomical and pathological features of the patient as possible.

There are various medical imaging modalities like Computed Tomography (CT) or Magnetic Resonance Imaging (MRI). Traditionally, a radiologist would look at the scanned images slice by slice for diagnosis and try to imagine the three dimensional representation of the anatomical features. This is a time consuming procedure and requires the radiologist to have well-founded experience as well as a highly sophisticated understanding of human anatomy. Three Dimensional (3D) medical visualization can help to overcome this problem by providing a 3D representation of the patient's anatomy, which is constructed from medical image dataset (König, & Gröller, 2001).

This study focuses on treatment of abdominal aortic aneurysms. An aneurysm is an area of a localized widening of a blood vessel. If aneurysm occurs through aorta in abdomen, it is called an abdominal aortic aneurysm (AAA). Aneurysms are a health risk because they can burst, or rupture. Approximately one in every 250 people over the age of 50 will die of a ruptured AAA (Moore, H.D., & Sydney, M.B., 1967). The death can be avoided if an aneurysm is detected and treated before it ruptures.

Endovascular stent graft is a preferred treatment method of aortic aneurysms. It is hard to decide which stent graft is suitable for the aneurysm due to anatomic features. During decision-making, it is most desirable to have detailed information about the aorta and aneurysm. This study presents a 3D visualization tool to diagnose abdominal aortic aneurysms and gather essential aortic measurements for appropriate stent graft selection with enhanced measurement modules.

1.1 Background and Problem Definition

The aorta is the largest artery in human body, which carries blood away from heart. Aorta runs through the chest and reaches to abdomen; this part is called the abdominal aorta. The abdominal aorta supplies blood to the lower part of the body.

When a weak area of the abdominal aorta expands or bulges, it is called an abdominal aortic aneurysm. The pressure from blood flowing through abdominal aorta can cause a weakened part of the aorta to bulge, much like a balloon. A normal aorta is about an inch (or about two centimeters) in diameter. However, an AAA can stretch the aorta beyond its safety margin. Aneurysms are a health risk because they can burst, or rupture. A ruptured aneurysm can cause severe internal bleeding, which can lead to shock or even death.

Aortic aneurysms can develop anywhere through the aorta. The majority, however, are located along the abdominal aorta. Most (about 90%) of abdominal aneurysms are located below the level of the renal arteries, the vessels that leave the aorta to the kidneys. About two-thirds of abdominal aneurysms are not limited to just the aorta but extend from the aorta into one or both of the iliac arteries.

Aortic aneurysms are mostly observed at male patients after sixty years of age. Males are four-to six times more likely than females to be affected. Risk factors for aortic aneurysm include cigarette smoking, high blood pressure, high serum cholesterol and diabetes mellitus. The most common cause of aortic aneurysms is "hardening of the arteries" called arteriosclerosis. At least 80% of aortic aneurysms are from arteriosclerosis. The arteriosclerosis can weaken the aortic wall and the pressure of the blood being pumped through the aorta causes expansion at the site of weakness.

Endovascular stent graft is the most preferred treatment method of aortic aneurysms. Endovascular means that the treatment is performed inside body using long, thin tubes called catheters that are threaded through blood vessels. Endovascular abdominal aneurysm repair (EVAR) has proven to be a less invasive, with reduced postoperative morbidity and mortality rates and decreased intensive

care unit and hospital stay (Teufelsbauer, & et al., 2002; Matsumura, Brewster, Makaroun, Naftel, 2003; Chuter, & et al., 1996; Zarins, & et al., 1999).

However, it has become clear that EVAR can be associated with a substantial risk of complications that may compromise its durability (Kantonen, & et al., 1999; Stone, Hayes, Aburahma, & et al., 2005; Ernst, 1993; Waasdorp, & et al., 2005). Not all the patients with abdominal aortic aneurysms are suitable for EVAR and careful patient selection, particularly concerning unfavorable anatomy, can be regarded as the most important determinant of EVAR (Choke, & et al., 2006; Resch, & et al., 2000). Pre-procedural evaluation is needed to select inappropriate patients, to determine potential difficulties and to decide which stent graft to use (May, & et al., 1999; Slater, Harris, Lee, 2008).

Reliable morphological evaluations, especially proximal neck measurements, are emerging as one of the most important determinant of EVAR indication. Since visual feedback from inner structure of the human body is low, several imaging techniques such as Computed Tomography, Magnetic Resonance Imaging and ultrasonography (US) have been developed over years. CT is one of these imaging modalities. It has been used in medical area to assist physicians in diagnosing medical diseases (Kunio, 2006). Computed Tomography is a powerful nondestructive evaluation technique for producing 2D and 3D cross-sectional images of an object from flat X-ray images.

1.2 Contributions of Thesis

This thesis introduces an interdisciplinary study which computer science and interventional radiology involves. The main contributions of this thesis are:

- We have adapted segmentation algorithms and developed a 3D visualization tool for abdominal aortic aneurysms for physicians.
- We generated measurement methods to select appropriate patients and predict stent graft for EVAR process.
- We developed a web extension to generate 3D model of the aorta for further diagnosis on web and archiving.

The motivation of this study originated from the demand of a specialized tool for abdominal aortic aneurysm diagnosis and treatment. As mentioned before, CT images are commonly used to diagnose abdominal aortic aneurysms. In traditional aspect, a radiologist supposed to diagnose such data sets by looking at the scanned images slice by slice. It is hard to generate a relationship between nearly 300 slices only by visual inspection. A need arises for a more convenient method.

There are several tools in the area, which reconstructs the sampled information into a 3D representation. However, most of them are CT scanner bundled general-purpose software and not specialized for abdominal aortic aneurysms. This study presents a tool that provides an interface to apply segmentation methods over CT images and generate 3D model of the aorta. With the ability to visualize aorta in detail as a separate structure, 3D visualization is a valuable resource for the diagnosis and pre-processing step of the EVAR procedure.

Another contribution of this study is development of aortic measurement methods and adaptation to 3D visualization tool. Aortic measurements play an important role in classification of suitable patients for EVAR procedure. Some of the patients are not suitable for the operation due to physical characteristics of the aorta. If EVAR is applied to unsuitable patients, the stent graft may slip or become twisted leading to undesired complications. Physicians should determine which patient is eligible for the EVAR procedure. The classification is performed according to aortic measurements such as aneurysm diameter, aortic neck angle that are provided by the measurement module in the 3D visualization tool. Aortic measurements are not only used select patients; they are also used to predict the stent graft type and size. An endovascular stent graft is a tube composed of fabric supported by a metal mesh. Stent grafts are used to reinforce the weakened part of the aorta. If stent grafts are not applied, blood pressure and other factors can cause this weak area to bulge like a balloon and it can eventually enlarge and rupture. The physical characteristics of aneurysm help physicians to determine which stent graft should be selected for the patient.

In this study, a web extension for extended diagnosis over web and archiving patient data was presented. Nowadays, internet has become an important platform to

publish applications. Several applications are ported to internet. as a result, they are accessible from a web browser anywhere in the world. Development of the web extension arose from this motivation. This web extension provides 3D visualization of the aorta on a web page using VRML standard. Physicians have ability to store patient data to a database and reach them from anywhere with a VRML plug-in enabled web browser. Web extension also provides systematic recording of the patients' data.

1.3 Thesis Organization

This dissertation is divided into seven chapters. Chapter 1 covers the introduction, project objectives, scopes of work and overall thesis organization.

Chapter 2 presents abdominal aortic aneurysms. Basic knowledge about aneurysms and treatment methods are presented in this chapter. Parameters needed for EVAR is summarized and stent selection criteria are introduced.

Chapter 3 introduces related works in two categories. Related works about aortic parameters present importance of aortic measurements during diagnosis and treatment of abdominal aortic aneurysms. Related works about aneurysm diagnosis and treatment tools present researches and software are available in the market.

Chapter 4 presents medical visualization methods. There are different imaging modalities to gather medical data. These modalities are explained in this chapter. Image Segmentation methods are also presented in this chapter. Chapter also includes data visualization methods to generate three dimensional models from segmented images.

In Chapter 5, an aortic aneurysm diagnosis and evaluation tool AMET is presented. AMET contains different modules. Each module explained in details and relationship between them is introduced. ACLP approach for aortic measurements is also presented in this chapter. AortaWeb is also presented in this chapter.

Chapter 6 contains test results to verify accuracy of the developed tool. Several evaluation methods were performed over data set generated by tool.

Chapter 7 includes the conclusions part. Contributions of the thesis and final remarks are presented in this chapter.

CHAPTER TWO

ABDOMINAL AORTIC ANEURYSMS

2.1 Abdominal Aortic Aneurysms

An abdominal aortic aneurysm is the enlargement of the lower part of the aorta that extends through the abdominal area. The aorta is the main blood vessel that carries blood from the heart to the rest of the body. Since arteries are elastic and are filled with blood under high pressure, the wall of the artery may become weakened and distended like a balloon. Abdominal aortic aneurysms (AAA) are a potentially lethal condition because of their likelihood of rupture (Treiman, & Bernhard, 1998). A normal aorta is about 1 inch (or about 2 centimeters) in diameter. However, an AAA can stretch the aorta beyond its safety margin as it expands. Aneurysms are a health risk because they can burst or rupture. A ruptured aneurysm can cause severe internal bleeding, which can lead to shock or even death.

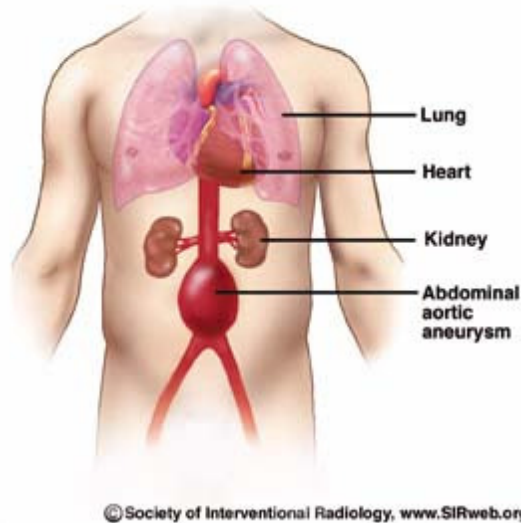


Figure 2.1 Location of abdominal aortic aneurysm
(Image Courtesy, Society of Interventional Radiology)

Aortic aneurysms can develop anywhere along the aorta. The majority, however, are located along the abdominal aorta. Most (about 90%) of abdominal aneurysms are located below the level of the renal arteries, the vessels that leave the aorta to the kidneys. About two-thirds of abdominal aneurysms are not limited to just the aorta but extend from the aorta into one or both of the iliac arteries (Figure 2.1).

An aneurysm is functionally defined as a focal dilation of an arterial segment to more than 1.5 times its normal diameter. The normal adult aortic diameter is approximately two cm. AAAs are often defined in the literature as aortic segments larger than 3 cm in diameter (Perler, & Becker, 1997).

The risk of rupture for an AAA over five cm in diameter is approximately 20%, over six cm approximately 40%, and over seven cm over 50%. Rupture of an AAA carries a risk of death up to 90% (Clouse, W.D., & et al. , 1998).

Males are four-to six times more likely than females to be affected. In men the onset of AAAs occurs at age 50, reaching a peak incidence at age 80. On the other hand women exhibit a delay in onset, generally beginning at age 70, with a peak incidence at age 90 (Perler, & Becker, 1997).

Risk factors for aortic aneurysm include cigarette smoking, high blood pressure, and high serum cholesterol. Smoking is associated with a 3- to 5-fold increase in the prevalence of abdominal aortic aneurysms (Fleming C., & et al., 2005). People with other medical conditions, such as coronary heart disease and peripheral vascular disease, are more likely to develop AAAs. A family history of abdominal aneurysm increases the risk of developing the condition and interacts with the risks associated with age and gender.

The most common cause of aortic aneurysms is "hardening of the arteries" called arteriosclerosis. At least 80% of aortic aneurysms are from arteriosclerosis. The arteriosclerosis can weaken the aortic wall and the pressure of the blood being pumped through the aorta causes expansion at the site of weakness.

AAA is often called a "silent killer" because there are usually no obvious symptoms of the disease. Three out of four aneurysms show no symptoms at the time they are diagnosed. They are often incidentally discovered when abdominal ultrasounds and/or CT scan studies are ordered for other conditions such as abdominal pains.

2.2 Diagnosis of Aneurysm and Treatment Methods

Aortic aneurysms are often found by chance during a physical examination, abdominal Ultrasound (US), Computed Tomography, Magnetic Resonance Imaging or echocardiogram performed for another reason, such as chest or abdominal pain.

(Chervu, & et al., 1995) found that only 38% patients had their AAAs initially detected by physical examination. The remainder (62%) was found incidentally on radiologic examinations performed for other indications.

Ultrasonography generally generates a clear picture of the size of an aortic aneurysm and has a high accuracy in measuring the size of the. However, ultrasound cannot accurately define the extent of the aneurysm and is inadequate for surgical repair planning. Ultrasonography was the standard method of screening and monitoring AAAs that have not ruptured.

Both computerized tomography and magnetic resonance imaging seem to be effective for diagnosis. Nevertheless, CT has become a standard in diagnosis of abdominal aortic aneurysms and used as data source in this interdisciplinary study. Computerized tomography of the abdomen is highly accurate in determining the size and extent of the aneurysm, and its relation with the renal arteries. Recent advances in CT imaging technology, such as helical CT and CT angiography, offer significant advantages over traditional CT.

Computerized tomography uses high doses of radiation and for evaluation of blood vessels, requires intravenous dye. This carries some risk including allergic reaction to the dye and irritation of the kidneys. In patients with kidney diseases, the doctor may consider an MRA (magnetic resonance angiography), which is a study of the aorta and the other arteries using MRI scanning.

CT is a good choice for preoperative planning in the diagnosis of abdominal aortic aneurysms. CT provides a detailed structure of the aneurysm and its extents. Detailed anatomy of the aneurysm provides accurate measurements that are crucial for the endovascular repair. Diameter of the aneurysm, diameter of the aortic neck, distance

from aortic bifurcation area are accurately provided by computed tomography. (Gravereaux, & et al., 2001; Bertges, & et al., 2003).

2.2.1 Treatment Methods

There are three well-known treatment options for abdominal aortic aneurysms: watchful waiting, surgical repair and endovascular stent graft repair. In watchful waiting, small aneurysms that are not rapidly growing or causing symptoms have a low incidence of rupture. They often do not require a treatment other than "watchful waiting" under the guidance of a vascular disease specialist. This includes generally follow-up ultrasound exams to determine aneurysm is stable.

Another treatment method is open surgical repair of aneurysm by a vascular surgeon. Open surgical aneurysm repair involves direct operative exposure of an aortic aneurysm, with replacement of the aneurismal segment of aorta with a graft made of artificial material. This procedure involves an incision from just below the breastbone to the top of the pubic bone. The aorta is clamped off above and below the aneurysm, the aneurysm is opened, and the graft directly sewn to the aorta above and below the aneurysm (Dillon, & et al., 2007).

This graft acts as a bridge for the blood flow. The blood flow then goes through the plastic graft and no longer allows the direct pulsation pressure of the blood to expand the weak aorta wall. The goal of the surgical treatment of abdominal aortic aneurysm is to prevent aneurysm rupture. Open surgical aneurysm repair is performed under general anesthesia. Depending on the extent of the procedure, the operation takes two to four hours. Most patients are hospitalized for five to seven days following surgery. This major operation usually requires about three months for full recovery.

Endovascular stent graft is the most preferred treatment method of aortic aneurysms (Ernst, 1993; Waasdorp, & et al., 2005). In endovascular abdominal aneurysm repair (EVAR), the treatment is performed inside body using long, thin tubes called catheters that are threaded through blood vessels. EVAR has proven to be a less invasive and decreased intensive care unit and hospital stay (Choke, & et

al., 2006). Endovascular repair is an effective treatment that can be performed safely, resulting in lower morbidity and lower mortality rates than those reported for open surgical repair (Ham, & et al., 2005; Cao, & et al., 2002; Malina, & et al., 1997).

Endovascular aneurysm repair (EVAR) was first pioneered in the early 1990s. The first idea of stent-grafts for treatment of aortic aneurysms was presented when the first trials in humans were reported in 1991 (Parodi, Palmaz, Barone, 1991). A stent graft is a tubular device, which is composed of special fabric supported by a rigid structure, usually metal. Stent grafts are used to support weak points in arteries (Figure 2.2). The stent graft acts as a false lumen for blood to travel through, instead of flowing into the aneurysm sack.

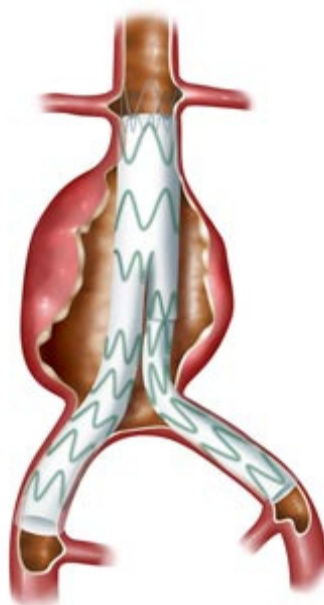


Figure 2.2 Abdominal aortic aneurysm with endovascular stent graft (Image Courtesy, Medtronic)

EVAR is performed by interventional radiologists and vascular surgeons. Stent-grafts are made in a number of configurations. The most common configuration is a bifurcated graft extending from the aorta into the common iliac or external iliac arteries. This typically requires access via both common femoral arteries. The main body is deployed first, followed by the iliac limbs. The materials used in the stent-graft vary with each manufacturer but most grafts are made of expanded

polytetrafluoroethylene or woven polyester, and most stents are made of nitinol or stainless steel.

Advantages of EVAR are listed as follows :

- ✓ No abdominal surgical incision
- ✓ Sutures only at the groins
- ✓ Faster recovery, shorter time in the hospital
- ✓ No general anesthesia
- ✓ Less pain
- ✓ Reduced complications

On the other hand, it has some disadvantages. Since the physicians have only CT images of the area, it is hard to predict which type and size of stent for aneurysm. In addition, there may be a possible movement of the graft after treatment, with blood flow into the aneurysm and resumption of risk of growth/rupture of the aneurysm. These disadvantages force physicians to prepare a well-planned procedure.

The key to successful EVAR is proper pre-procedural planning. Not all aneurysms are suitable for EVAR, depending on the anatomy of the aneurysm and iliac vessels. For those deemed suitable, careful aneurysm measurements will ensure the graft is the correct length and diameter. If the graft is too short the aneurysm will not be excluded from the circulation; if it is too long important branch vessels may be inadvertently occluded; and if it is too narrow in diameter there will not be an adequate seal against the aortic wall which may result in an endoleak.

The most important complication of abdominal aortic aneurysm repair is endoleak, in which there is persistent blood flow outside the graft but within the aneurysm sac. Depending on endoleak type, there is an ongoing potential for aneurysm expansion or rupture. Endoleaks are due to incomplete sealing, or exclusion of the aneurysm sac, and thus cause reflux of blood flow into the sac. Four types of endoleaks are currently known and labeled (Mandziak, & et al., 2004).

Type I endoleak is the blood flow into the aneurysm sac due to incomplete seal or ineffective seal at the end of the graft. This type of endoleak usually occurs in the early course of treatment, but may also occur later. Type II endoleak is blood flow into the aneurysm sac due to opposing blood flow from collateral vessels. In some circumstance when there are two or more patent vessels a situation of inflow and outflow develops creating an actively blood flow within channel created within the aneurysm sac. Type III endoleak is blood flow into the aneurysm sac due to inadequate or ineffective sealing of overlapping graft joints or rupture of the graft fabric. Again, this endoleak usually occur early after treatment, due to technical problems, or later due to device breakdown. Type IV endoleak is blood flow into the aneurysm sac due to the porosity of the graft fabric, causing blood to pass through from the graft and into the aneurysm sac.

2.2.2 Patient Selection

EVAR is a less invasive alternative to open surgical repair of aortic aneurysms and it is associated with less mortality and morbidity, and quick patient recovery leading to shorter hospital stay when compared to conventional open repair.

Not all patients are suitable for endovascular repair of the aneurysm. A number of factors need to be carefully evaluated before considering patient. Anatomy of the aneurysm plays an important role in patient selection step. When considering patients for EVAR, patient with AAA should meet the standard indications for open surgical treatment (Upchurch, & Criado, 2008). According to “The Society for Vascular Surgery and the International Society for Cardiovascular Surgery Guidelines”, aneurysm diameter which is larger than 4.5 cm has low operative risk and 5.5 cm has an average or high operative risk in repair of abdominal aortic aneurysms.

The primary goal in abdominal aorta aneurysm treatment is to extend survival through the prevention of rupture. As mentioned earlier, the treatment options include the following (Al-Omran, & et al., 2004):

1. Open Surgical Repair
2. Endovascular Aneurysm Repair (EVAR)

3. Continued surveillance

Making a decision among the above options is based on patient factors, aneurysmal factors and resources. Patient factors include comorbidities, operative risk, life expectancy, patient preferences. A patient's life expectancy is a critical factor in deciding whether to proceed with the repair. Age, sex, and known comorbidities are taken into account in determining life expectancy. Although the physician may recommend a course of action in many instances, the decision to repair or observe aneurysms should be made with informed input from the patient and family.

Aneurysmal factors include risk of rupture and anatomic characteristics. Predictors of the aneurysm rupture are listed as follows:

- Diameter of the aneurysm: This is the most reliable predictor of rupture and risk of rupture increases appreciably with each increase in diameter.
- Expansion: Rapid expansion of AAA (>1 cm/year) is associated with increased rupture risk.
- Smoking: Cigarette smoking may increase the risk of rupture by 1.5- to 2.4-fold.
- Hypertension: Elevation in blood pressure is highly associated with an increased risk of rupture.
- Family history: The risk of rupture was shown to be higher in patients with a positive family history of AAA, and risk increases with the number of first-degree relatives affected.
- Chronic obstructive pulmonary disease.
- Aneurysmal shape: Saccular aneurysms were found to carry a higher risk of rupture.

Aorto-iliac anatomy and vessel wall characteristics may influence the risks anticipated with conventional AAA repair, as well as the suitability for endovascular repair. In addition, resource availability has been an underemphasized element of the decision-making process for aneurysm repair, particularly when EVAR was considered.

The process of patient selection for EVAR is very important and includes several steps (Upchurch, & Criado, 2008). Firstly, detailed patient history and physical examination are evaluated. Evaluation parameters are features of rupture such as aneurysm size, expansion rate, and risk of surgical treatment based on demographic factors, patient history and life expectancy. Following preoperative assessment, preoperative imaging is considered with high quality contrasted and non-contrasted thin slice CT scan of entire abdominal aorta from above celiac artery origin to the common femoral artery bifurcations. After that, the risks of EVAR based anatomical criteria and the patient's ability to comply with required follow-up are evaluated. Finally, the most appropriate treatment strategy is determined for each patient based on the relative risks and benefits of the available treatment strategies.

2.2.3 EVAR Parameters

The planning of endovascular repair of AAA puts greater requirements on preoperative imaging since it must provide accurate information on the morphological structure and quantitative dimensions of the arterial segments involved.

Due to insufficient visual feedback, stent selection is a difficult step of EVAR planning (Blum, & et al., 1997). Stents must be properly selected in order to provide a longer lifetime. Stent selection depends on the morphological structure of the aneurysm and its extents (Resch, & et al., 1999; Chaikof, & et al., 2002). Physicians should gather accurate measurements on the disease area. Various measurements are used in stent graft planning according to stent types. But there are agreed measurements that are used in stent graft planning. Cheng and Stanley listed aortic measurements used for stent grafts (Cheng, 2010; Stanley, & et al., 2001).

Table 2.1 Commonly used anatomical features for abdominal aortic aneurysm

L1	Proximal neck length
$\partial 1$	Proximal diameter
α	Supra-renal angle
β	Infra-renal angle
L2	Aneurysm length (Between the start point of the aneurysm and the aortic bifurcation)
L3	Length of each iliac segment
$\partial 2$	Diameter of each iliac segment

Proximal neck length (L1) is the distance from the lower renal artery to the start of the aneurysm. Proximal diameter ($\partial 1$) is calculated on the orthogonal cross sections of the neck (Filis, Arko, Rubin, Zarins, 2003). Aorta has three main segments. The first segment is the aorta above the renal arteries, the second is the aortic neck, and the last segment is the aneurysm.

The aortic neck is the anatomic segment of the aorta which lies between two segments. Three segments creates two angles. These are aortic neck angulations; supra-renal angle (α) and infra-renal angle (β). Supra – renal angle is the angle between proximal aneurysm neck and supra-renal aortic axis. Infra – renal angle is the angle between proximal aneurysm neck and main axis of aneurysm (Figure 2.3).

Aneurysm length is the length between the start point of the aneurysm and the aortic bifurcation. In addition, length between the lowermost renal artery and the aortic bifurcation is important for determination of stent length. Iliac diameters ($\partial 2$) are calculated on the orthogonal cross sections of iliac arteries.

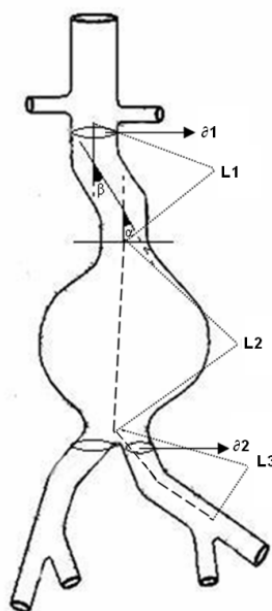


Figure 2.3 Anatomical features illustrated

Anatomical features that are used for EVAR decision and prediction of stent type and size are depicted in Figure 2.3. As mentioned earlier, not all of the patients are suitable for endovascular repair and these features need to be carefully evaluated before considering patient. If patient is eligible for endovascular repair, type and size of the stent graft should be considered.

2.3 Measurement Steps in Radio Diagnostic Department

Medical data used in this study was provided by Dokuz Eylul University Radio Diagnostic Department and measurement results of the study were compared with the methods applied in the department. The measurement methods used in the radio diagnostic department are proven to be prosperous due to success in the stent graft repair operation. The stent grafts are selected according to these measurement methods and stent-applied patients are avoided from the rupture of the aneurysm. Therefore, firstly the measurement steps in the radio diagnostic department should be considered.

In radio diagnostic department, aneurysm neck angulations are examined over MPR (Multi-Planar Reformatting) images at the region where aneurysm has the significant angulations. Several measurements were obtained from different cross-

sections to detect the exact value of angulations. The diameter of the neck is measured on the orthogonal cross – section of the neck. Several measurements of aortic neck diameter may be obtained at different viewpoints. Physicians have to select correct viewpoint to find the maximum neck diameter of the orthogonal cross-section just below the renal artery. As mentioned before, the proximal neck length is calculated between the lowermost renal artery and the start point of the aneurysm. Aneurysm length is the length between the start point of the aneurysm and the aortic bifurcation (Lederle, & et al., 1999).

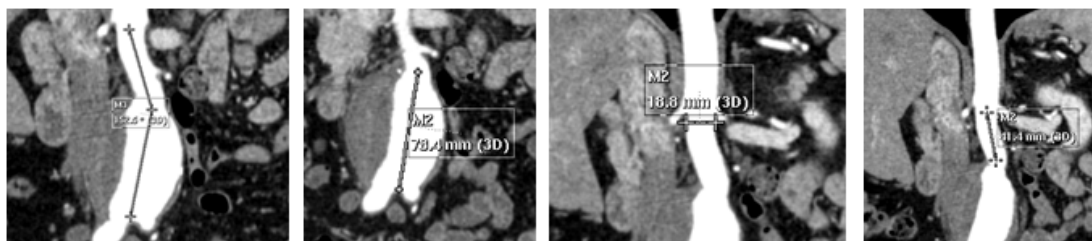


Figure 2.4 Aortic parameters: (1) Supra-renal (α) aortic angulation (2) Aneurysm length of the AAA (3) Neck diameter (4) Proximal neck length of the AAA

Multi-planar reformatting is a technique used in two-dimensional tomographic imaging (computed tomography and magnetic resonance) to generate sagittal, coronal, and oblique views from axial sections. Steps of currently used method show that physicians should spend effort to find the correct view of the MPR image. This brings up an operator-dependency problem. Also with non-specialized tools, measurements will not be in 3D depth leading to inconsistent results.

Although well-known post-processing applications are able to provide 3-D reconstructions of the aorta, these applications are not specialized for abdominal aortic aneurysms. Consequently obtaining a smooth abdominal aortic model may become a time consuming process. Physicians may obtain different aortic neck angles from different cross sectional MPR images leading to inconsistent results and should choose the correct sagittal, coronal or oblique slice in conventional method for reliable results. As a result, a specialized pre-processing platform is required to avoid operator-dependency for the arterial anatomy measurements. Abdominal Aortic Aneurysm Measurement and Evaluation Tool” (AMET) was developed to fill the gap in this area.

3D reconstruction with CT bundled software is another method used in the department. Most CT scanners are bundled with 3D reconstruction software to segment the structures of the body and visualize them. But these reconstruction software are mostly used to generate a general view of the internal organs. Further measurement capabilities are not provided. To gather measurements from generated models need extra effort.

CHAPTER THREE

RELATED WORKS

3.1 Related Works : Aortic Parameters

Several studies have reported that adverse proximal aortic necks were correlated with adverse outcomes. Many researchers have showed the associations between anatomic features and stent graft repair success. (Hovsepian, & et al, 2001) used the AneuRx device and found that short proximal neck was significantly associated with an increase complications and death (Hovsepian, & et al, 2001). (Stanley, & et al, 2001) found that risk of proximal endoleak increased with every millimeter of decrease in neck length less than 20 mm. (Dillavou, & et al., 2003) et al. showed the neck anatomy is the major determinant for suitability of patients for endovascular repair.

(Parodi, Palmaz, Barone, 1991) has reported that for perfect stent fixation the length and the diameter of the proximal aortic neck and distal iliac arteries have to be precisely known. (Aarts, & et al., 1999) reported their experiences that neck length and iliac arteries diameter are essential for successive exclusion of the aneurysm. On the other hand, increasing degrees of aortic neck angulation have been associated with adverse outcomes following endografting for AAA. (Sternbergh, 2002) described their experience with the AneuRx endograft and showed that aortic neck angulation appears to be an important determinant of outcome after EVAR.

(Robbins, & et al., 2005) examined the association of one such anatomic factor, proximal aortic neck angulation, with the incidence of adverse events following EVAR. Also (Albertini, & et al., 2000) showed a direct association between aortic neck angulation and adverse outcomes. (Rockman, & et al., 2002) reported their experience showing the association between endoleaks and aortic neck angulation.

All these study showed that determination of aneurysm morphology is very important for patient evaluation and selection before endovascular planning. In addition, aortic parameters are necessary for stent graft repair process. Stent size and type are determined according to these parameters.

3.2 Related works: Aneurysm Diagnosis And Treatment Tools

Several diagnostic procedures depend on medical images. These medical images are acquired from scanners in slices. Slices are not understandable if examined one by one. In order to overcome this problem, 3D volumetric structures are constructed according to intensity differences from slices. Image segmentation and 3D reconstruction techniques have accelerated 3D modeling in medical area. 3D visualization and evaluation became a key factor in diagnosis (Stytz, & Frieder, 1991).

Medical image supplier scanners are generally shipped with bundled 3D reconstruction software. However, these software are not specialized for a particular purpose. To diagnose aorta, all other body tissues should be eliminated to gather a clear model of the area. Bundled software generally includes other tissues and bones in models. Having a clear model is crucial for the physicians for an effective diagnosis.

There are several commercial solutions for aneurysm diagnosis and endograft planning. These are Materialise Mimics (Linninger, & et al., 2005), M2S Preview, TeraRecon Aquarius Intuition (Lee, 2010) and Slicer (Wolf, & et al., 2005).

3.2.1 Materialise Mimics

Mimics is an image processing software package for 3-dimensional design and modeling, commercially developed by Materialise NV. Mimics generates and modifies surface 3D models from stacked medical images such as Computed Tomography, Confocal Microscopy, Micro CT, and Magnetic Resonance Imaging through image segmentation.

Mimics is not a specialized visualization tool for only aortic aneurysms. It also is used to generate visualization for surgical simulation. Mimics provides segmentation and measurement tools for generated 3D models. Mimics is useful in helping physicians visualize the diseased AAAs. It has reconstruction methods and basic measurement tools to evaluate the AAA's morphology. The software allows

specialists to calculate some EVAR parameters such as length, distance, diameters (Figure 3.1). These parameters are important during planning of stent grafts.

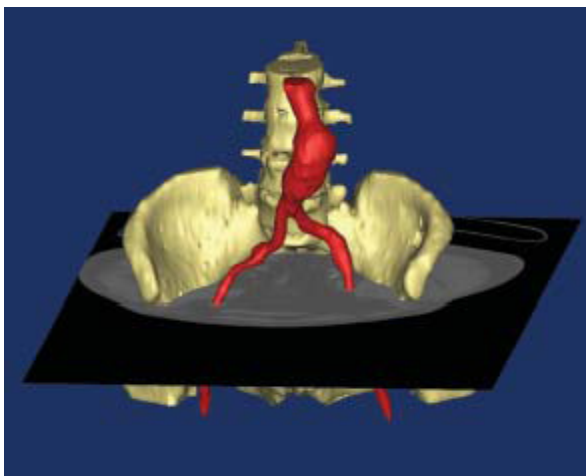


Figure 3.1 Materialise Mimics (Image Courtesy, Materialise)

Mimics includes several visualization functions such as contrast enhancement, panning, zooming and rotating of the 3D view. In Mimics, segmentation masks are used to highlight regions of interest.

3.2.2 M2S Preview

M2S Preview Treatment Planning Tool helps physicians and researchers visually preview and plan a wide range of disease procedures. This service includes 2D and 3D viewing, extensive measurement tools and manufacturer-specific endovascular virtual grafts to simplify treatment planning. M2S Preview Treatment Planning Tool supports following features:

- ✓ 3D modeling and reconstructions
- ✓ measurement tools, including diameter, lengths, volumes (blood, thrombus, calcified plaque)
- ✓ Simultaneous 2D slice and 3D model viewing
- ✓ View anatomical components within the lumen separately or as a whole, including blood flow, calcified plaque, thrombus, endoleaks, and dissections

Raw scan data is extracted from computed tomography scans, MRI, or other sources, and rendered by Preview into a three-dimensional (3D) format. M2S services include 2D and 3D viewing, measurement tools (including diameter, length, volumes) for endovascular treatment planning.

3.2.3 TeraRecon Aquarius Intuition

TeraRecon is a visualization and decision support technologies company. TeraRecon technology solutions provide advanced 3D imaging systems for medical and industrial applications. TeraRecon undertook development of volume-rendering technology and other post-processing techniques for incorporation into the company's post-processing workstation, Aquarius, the first of the company's "end-user" products (Figure 3.2).



Figure 3.2 Stent Graft Planning (Image Courtesy, TeraRecon)

Aquarius Intuition provides a cardiovascular analysis solution. Automated software identifies vasculature, quantifies aneurismal disease and supports detailed measurement of vessel dimensions and relative locations.

Aquarius Intuition also offers planning tools for endovascular intervention, especially for aortic repair. The EVAR planning tools provide automated centerlines of the vasculature with anatomy ID labeling, determined fixation points and appropriate measurements. All these are then reported in the embedded thoracic and abdominal endograft templates. Post-operative evaluation can be achieved with customized 3D templates that can help identify aneurysm growth and the integrity of implanted devices.

3.2.4 3D Slicer

3D Slicer is a free, open source software package for visualization and image analysis. The platform provides functionality for segmentation, registration and three-dimensional visualization of multi-modal image data, as well as advanced image analysis algorithms for diffusion tensor imaging, functional magnetic resonance imaging and image-guided therapy. Standard image file formats are supported, and the application integrates interface capabilities to biomedical research software and image informatics frameworks.

3D Slicer provides measure certain features on generated 3D model. This measurement capability may be used for endovascular treatment planning. However, this software package is not specialized for abdominal aortic aneurysm and measurement methods are not aortic feature based.

3.3 Deficiencies of Current Methods

Several medical image visualization tools have been developed to represent patient data in a visual form, to improve the comprehensibility and to facilitate processing of data. Materialise Mimics, M2S Preview, TeraRecon Endograft Planning, and Slicer came on the scene with this motivation to diagnose aneurysms. Slicer, is not specialized tool to diagnose aneurysms. Nevertheless, physicians are still able to visualize the aorta on the generated model. On the other hand,

Materialise Mimics, M2S Preview, TeraRecon Endograft Planning are designed for aortic aneurysms. However, all of them work only on windows platform and no operating system flexibility exists. Besides, TeraRecon Endograft Planning is a service-based solution where dataset should be uploaded to their server. The processed data is sent back and only evaluated by specified client software.

Since most of the examined tools are commercial products, they are large scale and complex systems that contain extra features that are not directly related to stent graft planning and stent selection parameters. Having extra features are not always desired in such decision support systems. Medical experts generally want to focus on the features that are directly related with their profession. Simple interfaces and step-based procedures make it easier to work on the medical data while extracting aortic features required for stent graft planning.

Furthermore, commercial products are not open source projects and they do not have the advantages such as extensibility and the right to use of the software in any way without limitation. The processed output data in such systems are exported with the limitations determined by the product supplier.

CHAPTER FOUR

MEDICAL VISUALIZATION

During the last 30 years, development of digital technology has influenced almost every aspect of our lives. They also have become more important in medical applications. Most of the medical imaging methods used today mostly relies on digital processing. Medical imaging is the technique and process used to create images of the human body for clinical purposes or medical science (Mustra, Delac, Grgic, 2008).

3D anatomic models obtained from medical images can be a powerful aid in the treatment of several medical situations. Medical data are obtained from imaging devices such as CT, MRI. After acquisition of data, regions are extracted using segmentation and registration image processing methods. Extracted regions are used as base data to construct 3D volumetric model of the body structures.

Because of there are several imaging equipment, it is very important to make a standard for connection and information exchange between medical appliances. There are many of manufacturers that make medical imaging equipment with different approaches, therefore, having a standard makes interchange of the images and medical data more easy. Digital Imaging and Communications in Medicine (DICOM) is a standard for handling, storing, printing, and transmitting information in medical imaging.

Usually, the methodologies used to obtain 3D models of an anatomic structure represented in medical images follow a sequence of three fundamental procedures (Pimenta, & et al. 2006):

- ✓ Acquisition of Medical Images
- ✓ Image Processing
- ✓ 3D Visualization

Each step is the complimentary of next step and is requisite for 3D anatomic structure construction. Figure 4.1 depicts the medical visualization sequence in details.

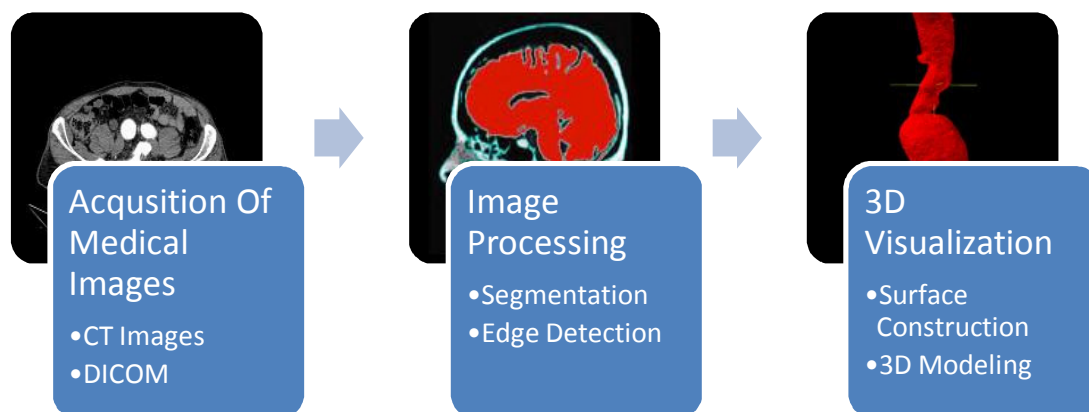


Figure 4.1 Medical Visualization Sequence

4.1 Acquisition of Medical Images

As the first stage of the process, the acquisition of medical images has an affective role in the result. The quality of the images of the structure to be reconstructed will dictate the success of the segmentation process, which is a critical stage of the complete procedure.

Data acquisition is the process of sampling physical conditions and conversion of the resulting samples into digital numeric values that can be manipulated by a computer (Aach, & et al., 1999). In medical, data is acquired from imaging equipment in order to provide images of the human body. William Roentgen discovered the first imaging techniques developed for medicine, x-rays, in 1895, and they were first used in medicine in 1896. Early radiology was chiefly concerned with skeletal morphology. Traditional x-rays are recorded on film, but recent developments in digital imaging have led to x-rays images being stored digitally in a computer rather than on film. Several modern imaging modalities became available to be used in diagnosis and treatment.

4.1.1 Imaging Modalities

With the advances in medical technology over the past few decades, a simple X-ray is no longer the standard way for physicians to diagnose and treat diseases. Different modalities of medical imaging have emerged over the years. All modalities

have their own advantages and disadvantages (Lee A., Dec 2008). Physicians decide which modality should be selected in order to deliver the best care. X-rays, ultrasound and magnetic resonance are different kind of imaging modalities.

X-rays are waves that have a relatively high frequency along the electromagnetic spectrum. They are absorbed or transmitted by different body tissues in varying amounts, producing different shades of black and white on an x-ray image. In general, bone appears white, soft tissue appears gray, and air appears black. This involves an x-ray machine aimed at the patient's body with a recording plate positioned behind the region of interest. Once the machine delivers its radiation, the image is captured on the plate. This allows an expert to assess the bones for fractures, the abdomen for bowel obstruction, and the breasts for signs of cancer (mammography), among other applications. Computed Tomography is an X-ray based technique developed in the 1970s, and now in widespread medical use. The idea is to take many x-rays of the same slice of a body, from different angles. It is then possible to reconstruct these x-rays to give a comprehensive image of the slice; this reconstruction is a complex, computer-based task. This procedure is then repeated along several slices, to produce a three-dimensional image of a part of the body.

Ultrasound is a widely used, sound based technique. It measures the differences in echo properties of different organs, and can thus generate images simply by projecting sound into the body, and measuring how and what bounces back. The non-invasive and harmless approach has made ultrasound extremely popular in pregnancy scans.

Magnetic resonance imaging, unlike x-ray imaging, does not use radiation. Instead, MRI works based on magnetic waves and the spin of protons. Data is processed by a computer to form the images that clinicians use.

In this study, Multidetector CT examinations were performed by using a four-detector row scanner (Philips Medical Systems MX8000, the Netherlands). One hundred milliliters (300 mg of iodine per milliliter) of a non-ionic intravenous contrast material was administered, through a 20-gauge catheter inserted into an

antecubital vein, at a rate of 4 mL/sec by using a power injector. Arterial phase imaging was performed by using bolus tracking. CT parameters were set at 120 kVp and 180 mAs and a 1.00-mm detector configuration was used. Three-millimeter-thick sections were reconstructed and downloaded to the picture archiving and communication system.

4.1.2 DICOM File Format

Medical Images are stored as DICOM files in picture archiving and communication system. According to NEMA DICOM Standard Guide, DICOM is an image communication standard for medical devices. With the introduction of computed tomography followed by other digital diagnostic imaging modalities in the 1970's, and the increasing use of computers in clinical applications, the American College of Radiology (ACR) and the National Electrical Manufacturers Association (NEMA) recognized the emerging need for a standard method for transferring images and associated information between devices manufactured by various vendors.

DICOM Standard includes a file format definition and a network communications protocol. The communication protocol is an application protocol that uses TCP/IP to communicate between systems. DICOM files can be exchanged between two entities that are capable of receiving image and patient data in DICOM format. According to NEMA DICOM standard; it facilitates interoperability of medical imaging equipment by specifying:

- ✓ For network communications, a set of protocols to be followed by devices claiming conformance to the standard.
- ✓ The syntax and semantics of commands and associated information which can be exchanged using these protocols.
- ✓ For media communication, a set of media storage services to be followed by devices claiming conformance to the standard, as well as a file format and a medical directory structure to facilitate access to the images and related information stored on interchange media.



Figure 4.2 DICOM Image

A sample DICOM image is depicted in figure 4.2 in a selected frame. A DICOM data object consists of a number of attributes, including items such as name, ID, etc., and one special attribute containing the image pixel data. A single DICOM object can only contain one attribute containing pixel data. For many modalities, this corresponds to a single image. Dicom header describes the image dimensions and stores other text information about the scan.

Nearly 300 DICOM images are processed for each patient in this study. Interventional Radiology Department of Dokuz Eylül University Faculty of Medicine provided all DICOM data for several patients.

In computer tomography diagnostics, the measured Hounsfield units (HU) are used to characterize tissue and are in that respect compared to nominal HU values found in the radiological literature. (Sande, Martinsen, Hole, Olerud, 2010) The Hounsfield scale, is a quantitative scale for describing radiodensity. CT machines were the first imaging devices for detailed visualization of the internal three-dimensional anatomy of living creatures, initially only as tomographic reconstructions of slice views or sections. Since the early 1990s, with advances in computer technology and scanners using spiral CT technology, internal three-dimensional anatomy is viewable by three-dimensional software reconstructions, from multiple perspectives. By comparison, conventional X-ray images are two-dimensional projections of the true three-dimensional anatomy, i.e. radio density shadows.

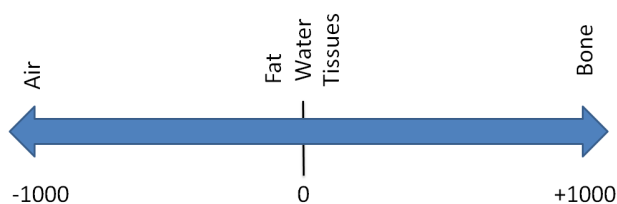


Figure 4.3 Hounsfield Scale

Specifically, Hounsfield defined zero Hounsfield units (HU) as the radio density of distilled water at standard pressure and temperature, and -1000 HU as the radio density of air (Figure 4.3). The Hounsfield number of a tissue varies according to the density of the tissue (Hounsfield, 1980). The DICOM image pixel values represent Hounsfield numbers.

The use of this standardized scale facilitates the intercomparison of CT values obtained from different CT scanners and with different X-ray beams energy spectra, although the CT number of materials whose atomic composition is very different from that of water will be energy dependent.

4.2 Image Processing

Digital image processing is a technique in which the data from an image are digitized and various mathematical operations are applied to the data, generally with a digital computer, in order to create an enhanced image that is more useful or pleasing and perform some of the interpretation and recognition tasks. In medical data visualization, image processing plays a crucial role, since medical data are stored as image files.

Image processing techniques that are applied or examined in this study are explained in following sections. One of the important prerequisite for visualization is the availability of segmentation methods that identify and classify interesting features in the data set.

4.2.1 Segmentation

In computer vision, segmentation refers to the process of partitioning a digital image into multiple segments. These segments are sets of pixels. The goal of

segmentation is to simplify and change the representation of an image into something that is more meaningful and easier to analyze. Image segmentation is generally used to locate objects and boundaries in images. These boundaries include lines, curves or contrast differences. More precisely, image segmentation is the process of assigning a label to every pixel in an image such that pixels with the same label share certain visual characteristics (Shapiro, Stockman, 2001).

The result of image segmentation is a set of segments that collectively cover the entire image, or a set of contours extracted from the image. Each of the pixels in a region are similar with respect to some characteristic or computed property, such as color, intensity, or texture. Adjacent regions are significantly different with respect to the same characteristics.

Several general-purpose algorithms and techniques have been developed for image segmentation. Since there is no general solution to the image segmentation problem, these techniques often have to be combined with domain knowledge in order to effectively solve an image segmentation problem for a problem domain.

Segmentation could be performed manually or automatically. Manual segmentation consists of the manual drawing of the shape to be extracted from each medical image. This process can make use of the tools provided by specific software for analysis of medical images, but the effort to identify the contours is completely done manually. Therefore, this technique is very flexible, but it demands a high work force that might not be always available.

Automatic segmentation avoids the greatest part of the manual process, as it appeals to the properties of the image to perform the identification of the shape to extract.

Some of the practical medical applications of image segmentation are listed as follows:

- ✓ Locate tumors and other pathologies
- ✓ Measure tissue volumes
- ✓ Computer-guided surgery

- ✓ Diagnosis
- ✓ Treatment planning
- ✓ Study of anatomical structure

This study is related with last three items in the list. The study proposes a diagnosis and treatment planning tool which also studies anatomical structure of the aorta which developed an aneurysm.

4.2.2 Clustering Methods

(Haralick, Shapiro, 1985) presented that the difference between clustering and segmentation is that in image segmentation, grouping is done in the spatial domain of the image, while clustering is done in measurement space. It is also possible for clustering to result in overlapping regions, while that is not the case for segmentation results. Clustering and spatial segmentation can be combined to form spatial clustering, which combine histogram techniques with spatial linkage techniques for better results.

The K-means algorithm is an iterative technique that is used to partition an image into K clusters. The basic algorithm is:

- ✓ Pick K cluster centers, either randomly or based on some heuristic
- ✓ Assign each pixel in the image to the cluster that minimizes the distance between the pixel and the cluster center
- ✓ Re-compute the cluster centers by averaging all of the pixels in the cluster
- ✓ Repeat steps 2 and 3 until convergence is attained (e.g. no pixels change clusters)

4.2.3 Histogram Based Methods

Histogram-based methods are very efficient when compared to other image segmentation methods because they typically require only one pass through the pixels. In this technique, a histogram is computed from all of the pixels in the image, and the peaks and valleys in the histogram are used to locate the clusters in the image (Shapiro, Stockman, 2001).

Color or intensity can be used as the measure. A refinement of this technique is to recursively apply the histogram-seeking method to clusters in the image in order to divide them into smaller clusters. This is repeated with smaller and smaller clusters until no more clusters are formed.

4.2.4 Edge Detection Methods

Edge detection is a well-developed field on its own within image processing. Region boundaries and edges are closely related, since there is often a sharp adjustment in intensity at the region boundaries. Edge detection techniques have therefore been used as the base of another segmentation technique.

The edges identified by edge detection are often disconnected. To segment an object from an image however, one needs closed region boundaries.

There are many ways to perform edge detection. However, the majority of different methods may be grouped into two categories:

- Gradient: The gradient method detects the edges by looking for the maximum and minimum in the first derivative of the image.
- Laplacian: The Laplacian method searches for zero crossings in the second derivative of the image to find edges. An edge has the one-dimensional shape of a ramp and calculating the derivative of the image can highlight its location.

4.2.5 Region Growing Methods

Region growing algorithm is an effective approach for image segmentation (Horowitz, & Pavlidis, 1974). Region growing based approaches extract regions that satisfy a homogeneity criterion like gray level, color, texture, shape, spatial location.

The first region growing method is the seeded region growing method. This method takes a set of seeds as input along with the image. The seeds mark each of the objects to be segmented. The regions are iteratively grown by comparing all unallocated neighbouring pixels to the regions. The difference between a pixel's

intensity value and the region's mean, δ , is used as a measure of similarity. The pixel with the smallest difference measured this way is allocated to the respective region. This process continues until all pixels are allocated to a region.

The basic formulation for Region Growing Segmentation is as follows:

- ✓ An initial set of small areas are iteratively merged according to similarity constraints.
- ✓ Arbitrary seed pixel is selected and compared with neighbouring pixels.
- ✓ Region is grown from the seed pixel by adding in neighbouring pixels that are similar. This process increases the size of region
- ✓ When the growth of one region finishes, another seed pixel which does not yet belong to any region is selected.

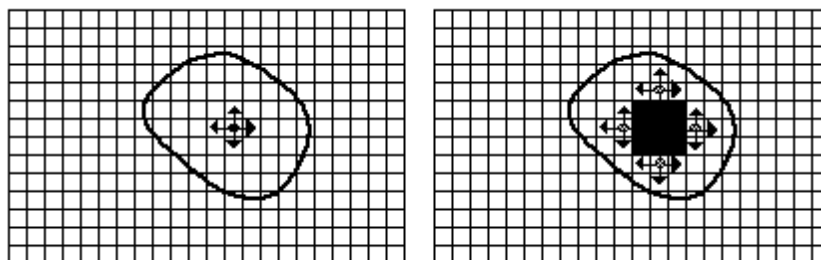


Figure 4.4 Region Growing Segmentation

Region growing segmentation procedure is depicted in figure 4.4. As mentioned before, there are several segmentation methods. Region growing approach is selected in this study to segment the aorta regions in order to build up a detailed 3D aorta model.

4.3 Data Visualization

Data visualization is the study of the visual representation of data. It is explained as the information, which has been abstracted in some schematic form, including attributes or variables for the units of information. In 3D computer graphics, 3D modeling is the basic step for data visualization. 3D modeling is the process of

developing a mathematical representation of any three-dimensional surface of object via specialized software. At the end of the process, a 3D model is created and it is displayed as a two-dimensional image through a process called 3D rendering.

3D models represent 3D objects using a collection of points in 3D space, connected by various geometric entities such as triangles, lines, curved surfaces, etc. Being a collection of data, 3D models can be created by hand, algorithmically or scanned. In this study, 3D models are generated from segmented DICOM images algorithmically.

Representation of 3D models is another concept. To visualize generated 3D models surface modeling techniques should be applied to data stored in 3D models. In surface modeling, polygons and triangles are used to compose images as three-dimensional in appearance in computer graphics. In 3D computer graphics, polygonal modeling is an approach for modeling objects by representing or approximating their surfaces using polygons.

4.3.1 Marching Cubes Approach

Marching cubes is a computer graphics algorithm, published in the 1987 SIGGRAPH proceedings by (Lorensen, Cline, 1987). It is used for extracting a polygonal mesh of an isosurface from a three-dimensional scalar field. The algorithm proceeds through the scalar field, taking eight neighbor locations at a time. This forms an imaginary cube. Then the polygons needed to represent the part of the isosurface that passes through this cube are determine. The individual polygons are fused into the desired surface.

There are pre-calculated array of 256 possible polygon configurations ($2^8 = 256$) within the cube, by treating each of the eight scalar values as a bit in an 8-bit integer. If the scalar's value is higher than the iso-value, then the appropriate bit is set to one, while if it is lower it is set to zero. The final value after all eight scalars are checked is the actual index to the polygon configuration array. Finally, each vertex of the generated polygons is placed on the appropriate position along the cube's edge by linearly interpolating the two scalar values that are connected by that edge.

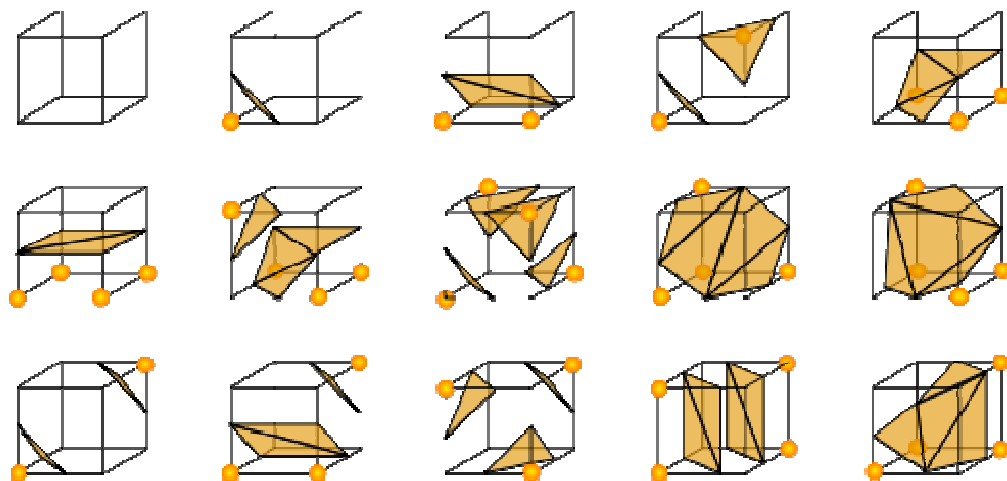


Figure 4.5 Marching cubes unique configurations

The pre-calculated array of 256 cube configurations can be obtained by reflections and symmetrical rotations of 15 unique cases (Figure 4.5). The applications of this algorithm are mainly concerned with medical visualizations such as CT and MRI scan data images.

4.3.2 Fair Tiling Approach

Even though, “Marching Cubes” approach is a generic and successful algorithm to generate surfaces of irregular objects; it sometimes has a high computation time. While this study is interested in abdominal aorta model, which is a tubular structure, a specialized and faster method has been developed. “Fair Tiling” surface generation method was developed for 3D visualization of vascular structures generated from medical images (Utku & et al. 2010).

Fair Tiling Method is based on forming the least triangular structure from coordinates corresponding to the mutual cross-sectional by distributing point values in consecutive sections. Consecutive sections are similar in shape; therefore, each vertex on the perimeter of the section corresponds to vertices of the other section. Unlike marching cubes approach, the vertices of the polygons to be formed are approximately definite. The main idea behind fair tiling approach is the generation of scanning triangular areas between the middle point of the sections and the vertices of the sections. Generated triangular structure includes intersecting points on scanning

area. In this study, sections are expressed as aortic-segmented regions from CT images.

As mentioned earlier, nearly 300 CT images are processed to generate the surface and whole model of the aorta. After segmentation process, each segmented region is in the form of a circular structure. Outer surface of the aorta is generated from the vertices of the segmented regions. Fair Tiling approach simply handles two consecutive segmented regions and discovers the vertices of the region, which corresponds to vertices of the next region. Figure 4.6 depicts the two consecutive regions and the connected vertices.

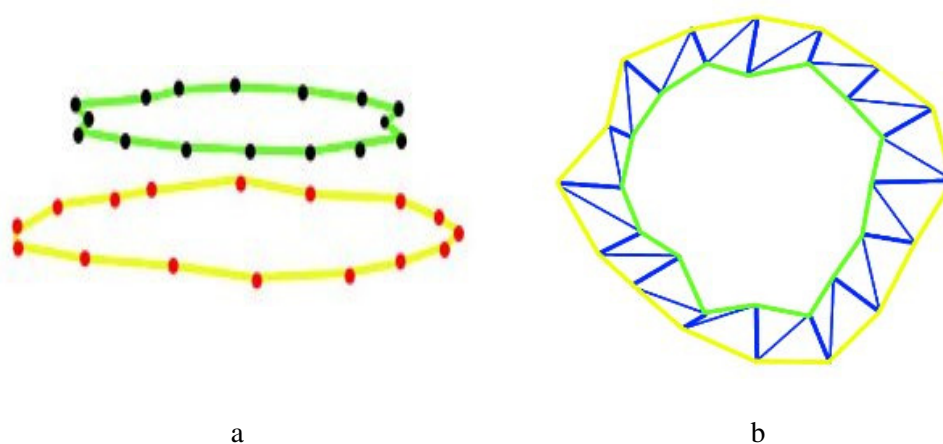


Figure 4.6 (a) Two consecutive region vertices (b) Connected vertices

Two important steps are prerequisite of Fair Tiling approach. These are edge detection and midpoint calculation. Vertices of the segmented regions are determined by edge detection methods that are previously explained in preceding chapters. The result of edge detection method is the vertices that will be the base data for Fair Tiling approach. A simple edge detection method was selected to extract the vertices from segmented regions. If the segmented region is considered as a bitmap image, vertices of the perimeter of the region correspond to a pixel (figure 4.7). Edge vertices are stored as Cartesian point coordinates of a 2D plot.

Middle point calculation is another prerequisite for Fair Tiling approach. Because the middle point of the regions are overlapped to generate the scanning triangular area. The middle point calculation of a region is also an important component of the developed tool and will be explained in details in next chapter.

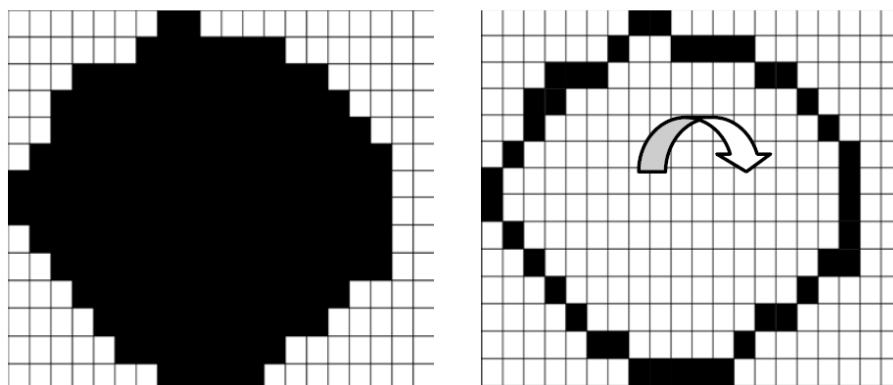


Figure 4.7 Edge detection is applied to segmented region

If the number of vertices on both regions is equal, it is quite easy to connect the vertices and generate polygons. On the other hand, if vertex number of the consecutive regions is not equal, there cannot be a one-to-one relationship between regions. We developed an algorithm to find the connections between the regions based on neighborhood approach. Two consecutive segmented region vertices are depicted in Figure 4.8.

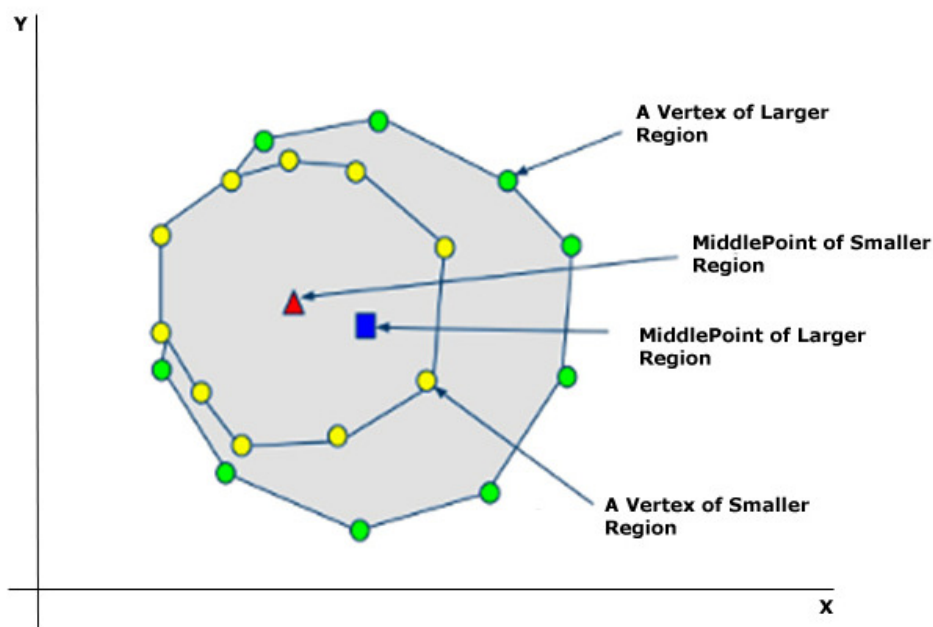


Figure 4.8 Two regions are overlapped

The middle points of the two consecutive segments are overlapped. This overlap mechanism works as follows:

- The number of vertices are considered to decide which segment vertices will be shifted.
- The segment with smaller number of vertices is considered as the base segment.
- The vertices of the larger segment are shifted to ensure the middle points are overlapped.

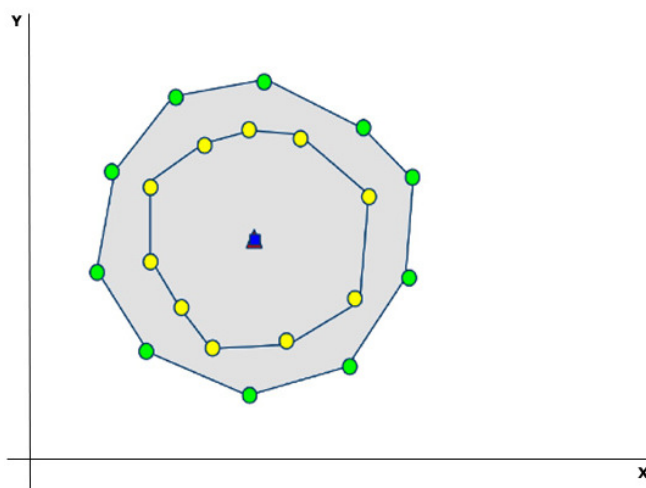


Figure 4.9 Overlapped segments

After the segments are overlapped (Figure 4.9), an imaginary circle that covers the both segments are considered. One vertex on the inner segment is selected as the initial point. The half way distance between selected vertex and the previous vertex is marked. Same procedure is performed for the selected vertex and next vertex. Two imaginary lines are drawn from the middle point to the marked points. The intersection of these lines with the imaginary circle forms a triangle. The vertices of outer region, which resides in this triangle, are the connection points of the initial vertex to form a polygon (Figure 4.10).

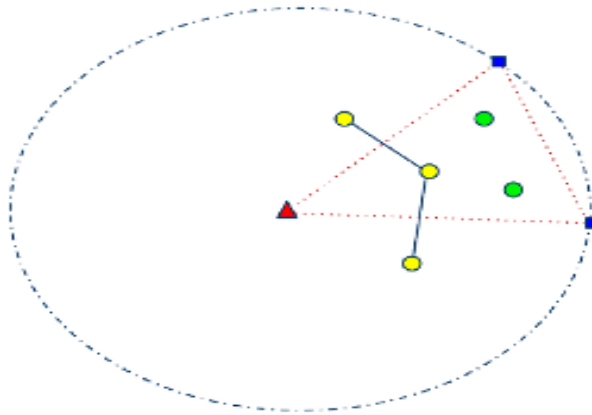


Figure 4.10 A triangle is formed using vertices of overlapped segments.

The vertices that reside inside a triangle are determined by Barycentric methods (Figure 4.11). Three Barycentric (Warren, Schaefer, Hirani, & Desbrun, 2006) coordinates are defined; α, β, γ

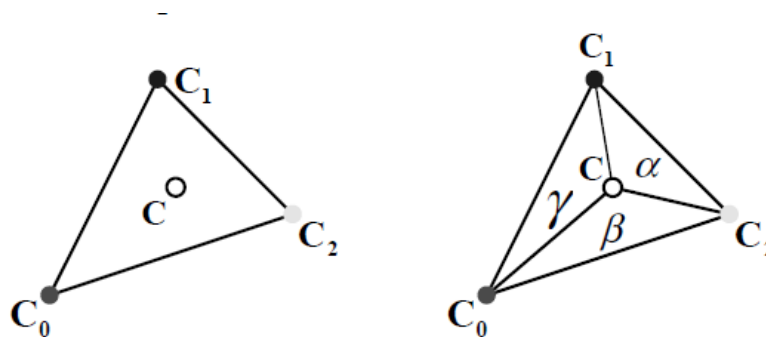


Figure 4.11 A point whether inside a triangle or not is determined by Barycentric method.

$$C = C_0\alpha + C_1\beta + C_2\gamma \text{ where } \alpha + \beta + \gamma = 1$$

$$C \text{ is inside } C_0C_1C_2 \Leftrightarrow \alpha, \beta, \gamma \in [0,1]$$

$$\alpha = \frac{\text{Area}(C C_1C_2)}{\text{Area}(C_0C_1C_2)} \quad (1)$$

$$\beta = \frac{\text{Area}(C_0 C C_2)}{\text{Area}(C_0 C_1 C_2)} \quad (2)$$

$$\gamma = \frac{\text{Area}(C_0 C_1 C)}{\text{Area}(C_0 C_1 C_2)} \quad (3)$$

The area of the triangle is calculated as follows;

$$X_1 Y_2 = C_{0x} \times C_{1y}$$

$$X_2 Y_3 = C_{1x} \times C_{2y}$$

$$X_3 Y_1 = C_{2x} \times C_{0y}$$

$$X_2 Y_1 = C_{1x} \times C_{0y}$$

$$X_3 Y_2 = C_{2x} \times C_{1y}$$

$$X_1 Y_3 = C_{0x} \times C_{2y}$$

$$A = \frac{1}{2}(X_1 Y_2 + X_2 Y_3 + X_3 Y_1 - X_2 Y_1 - X_3 Y_2 - X_1 Y_3) \quad (4)$$

Point C lies inside the triangle if and only if $\alpha, \beta, \gamma > 0$. Otherwise, C lies outside the triangle.

In left part of figure 4.12, vertices that are generated from nine segmented and edge-detection applied CT slices are displayed. Right part of figure 4.12 contains the polygon surface structure, which is constructed by Fair Tiling method.

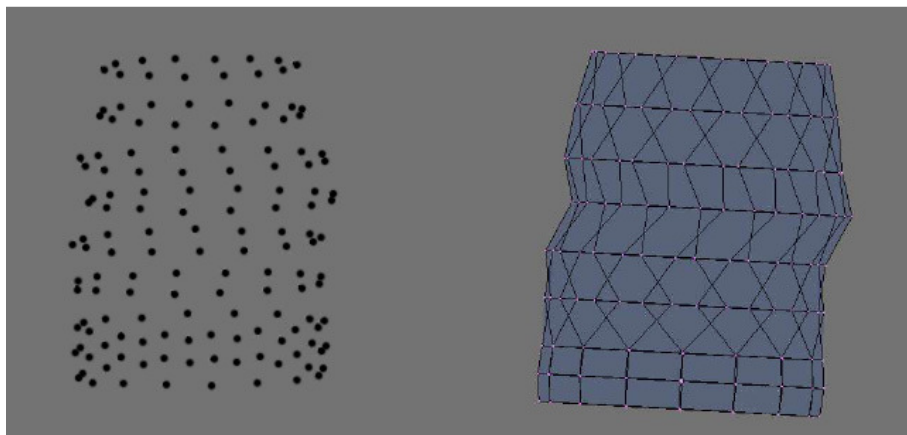


Figure 4.12 (Left) Boundary vertices (Right) Polygon surface Structure

General algorithms for fair tiling can be summarized as follows:

- Two consecutive slices are considered
- The slice with smaller number of edge points is set as reference. (Inner slice)
Two consecutive edge points in this reference slice is marked.
 - Center (delta point) of these points is determined.
 - An imaginary line is drawn from inner slice center to delta point.
 - Intersection points for the inner slice are stored in a special data structure. Imaginary line is used to find intersection points.
- For each point on the inner slice
 - Two stored points and one inner slice center creates a triangle
 - Each point on the outer slice is tested whether point is inside the triangle or not. If the point is inside the triangle, a triangle mesh created with these points.

4.3.3 Comparison of Fair Tiling and Marching Cubes Methods

Marching cubes is a successful method to generate the surface polygons of the objects from a given dataset. However, in some cases it requires high computation power to generate surface polygons. Especially, in real-time simulations, animation frame should be created immediately. Fair Tiling method was developed to generate the surface polygons of the tubular structures in a faster way. When medical area is considered, vessel-like structures are good examples that are constructed by Fair Tiling method.

In marching cube method, all object points are stored in a special three-dimensional data structure and index based search methods was applied through a lookup table, which uses unit cube points. Marching cube method is a generic algorithm and can be applied to any object. On the other hand, Fair Tiling uses simple method, which uses the perimeter vertices of the consecutive segments to generate the surface polygons. It is a specific algorithm for tubular structures. In this study, it was applied to generate the three-dimensional model of the aorta.

Another difference between Marching Cubes and Fair Tiling methods is the generated polygon numbers. Any object can be presented with different number of polygons. This difference comes out because of the method used in triangular creation process. In this study, we observed Fair Tiling method generated less number of polygons compared to Marching Cubes method.

Ten patients having abdominal aortic aneurysm disease were considered to compare the differences between two methods. Three-dimensional aorta model was generated using two different methods. Execution time and polygon number count was calculated to reflect the difference. Results are listed in Table 4.1.

Table 4.1 Comparison of Marching Cubes and Fair Tiling

	Execution Time (in milliseconds)		Number of Generated Polygons	
	Marching Cubes	Fair Tiling	Marching Cubes	Fair Tiling
1	174203	458	308146	128666
2	81645	181	152210	56496
3	97695	154	221060	49539
4	75064	118	127578	41143
5	99511	193	171692	60790
6	76926	101	123538	31696
7	90627	243	189842	65358
8	91844	251	217172	69838
9	80735	217	157774	57820
10	97229	258	224170	72730

The results show that Fair Tiling uses a faster method to generate surface polygons of the aorta. Generated three-dimensional aorta model contains fewer polygons in Fair Tiling method compared to Marching Cubes approach. The resulting aorta models in both approaches are displayed in Figure 4.13.

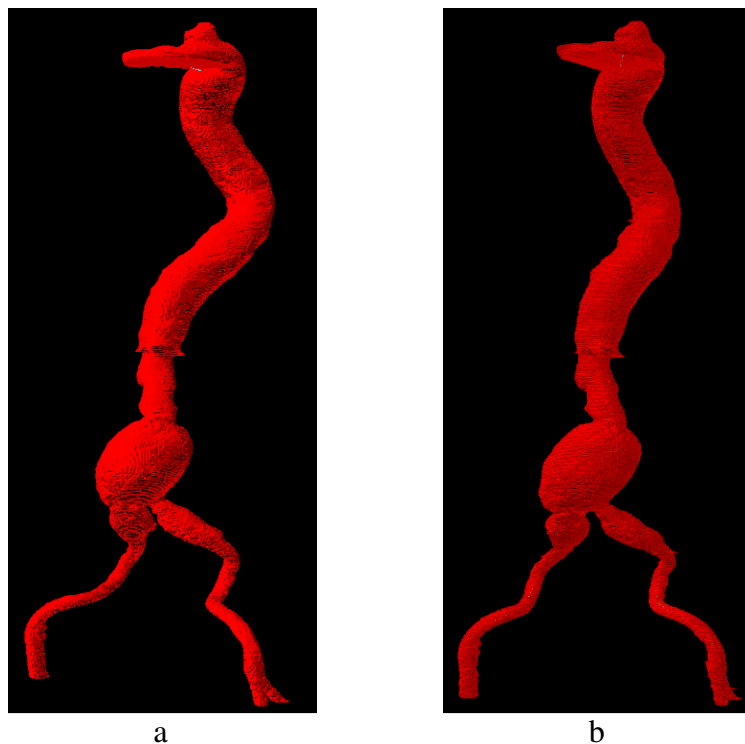


Figure 4.13: 3D aorta model generated by a) Marching Cube b) Fair Tiling

Marching cubes is a computer graphics algorithm that produces triangle mesh by computing iso-surfaces from discrete data. It is probably the most popular method for iso-surface extraction and rendering. To visualize the aorta, more uniform data is used, because aorta is a vessel and contains tubular structures. Fair Tiling approach is based on this idea. Both marching cubes and fair tiling algorithms are included in the aortic aneurysm measurement and evaluation tool that is presented in next chapter.

CHAPTER FIVE

ABDOMINAL AORTIC ANEURYSM MEASUREMENT AND EVALUATION TOOL

Decision-making is the study of identifying and choosing alternatives based on the values and preferences of the decision maker. Medical decision making often involves making a diagnosis and selecting an appropriate treatment method and procedures.

Proper selection of patient and stent-graft combinations in endovascular aneurysm repair (EVAR) depends on knowledge and experience with the different types of stents that have to be adapted to the patient's unique abdominal aortoiliac anatomy. The aim of this study was to analyze the consistency and variance in EVAR suitability assessment between clinicians (Rödel, & et al., 2006).

During decision making, to assist operators diagnosing abdominal aortic aneurysms, a specialized pre-processing “abdominal aortic aneurysm measurement and evaluation tool” was developed. Abdominal aortic aneurysm measurement and evaluation tool provides visual interfaces with broad measurement capabilities to generate 3D model of the aorta for a better diagnosis and accurate stent selection. This study is an interdisciplinary research where computer science and radio diagnostic department involved. The motivation behind the research is deficiencies of the currently used method in radio diagnostic department for endovascular stent graft repair.

5.1 Abdominal Aortic Aneurysm Measurement And Evaluation Tool

In this study, a specialized measurement and evaluation tool was developed for abdominal aortic aneurysm. The tool provides navigation and visualization of the aorta in 3D perspective. Axial images of the Multi Detector Computed Tomography (MDCT) examinations were downloaded to AMET to generate an automated analysis of aortic aneurysm neck angle and measurements. Downloaded images are in the Digital Imaging and Communications in Medicine (DICOM) standard.

AMET is used for making measurement and evaluation related with aortic dimensions and characteristics of aneurysm. It generates 3D Aortic model by processing these 2D DICOM CT pictures. Thereby, physicians can make essential evaluation and measurements reliably, readily and quickly by using this model.

As a diagnosis and treatment-planning tool, AMET has following features:

- ✓ Loading DICOM directory and viewing DICOM Slices
- ✓ Contrast and brightness enhancement
- ✓ Segmentation from seed points
- ✓ 3D Visualization of the aorta and its extents
- ✓ Measurement of aortic features

AMET is a step-based tool where each operation is a preprocess of the other. To achieve measurement features, all previous steps should be completed. In this manner, AMET can be explained in modules. AMET consists of several modules in an integrated environment:

- ✓ Dicom Viewer Module
- ✓ Aorta Segmentation Module
- ✓ 3-D Visualization & Observation Module
- ✓ Measurement and Evaluation Module

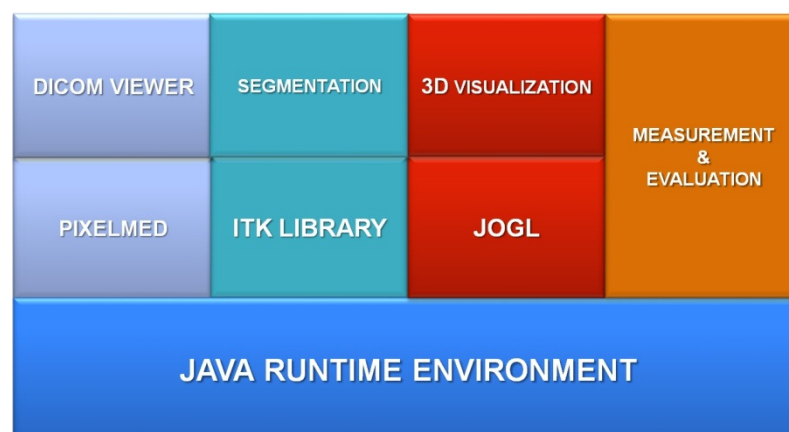


Figure 5.1 AMET Framework

The relationship between AMET modules is depicted in figure 5.1. In the figure, the libraries that are used in the module are shown.

5.1.1 Dicom Viewer

Dicom Viewer module plays a crucial role in pre-processing stage. It provides physicians to explore a set of DICOM images. DICOM files contain metadata that provide information about the image data, such as the size, dimensions, bit depth, modality used to create the data, and equipment settings used to capture the image. Since DICOM has become a standard in medicine, it is no longer a complex procedure to display DICOM images. There are several libraries to process DICOM files. DICOM viewer module of AMET was developed by using PixelMed toolkit. PixelMed is a stand-alone DICOM toolkit, which is used for reading and creating DICOM data. It supports directory browsing, image viewing, and DICOM object validation. The toolkit is open source and freely available for both non-commercial and commercial use, under BSD License. PixelMed provides java libraries to manage DICOM data. The DICOM viewer module of AMET provides following opportunities for managing DICOM images.

- ✓ Loading DICOM images
- ✓ Browsing DICOMDIR files in typical structure patient/study/series/study
- ✓ Standard navigation (pan, zoom, magnification)
- ✓ Advanced tools to measure area/distance
- ✓ Brightness and contrast adjustment with mouse movement
- ✓ Simultaneous visualization of multiple DICOM files.

DICOM Viewer module allows physicians to browse through slices and examine the CT images to decide which slices should be included in segmentation.

5.1.2 Aorta Segmentation

To extract a meaningful model from DICOM slices, an image processing technique, segmentation was applied to medical images. In each axial image, aorta is observed as a convex closed region. To determine the whole structure of the aorta, the boundaries of the closed region in each image should be obtained. Segmentation is used to locate objects and boundaries in images as an image processing technique.

More precisely, image segmentation is the process of assigning a label to every pixel in an image such that pixels with the same label share certain visual characteristics.

Several general-purpose algorithms and techniques have been developed for image segmentation. Region growing algorithm was used to extract aorta segments in this study by using ITK (Insight Segmentation and Registration Toolkit). It is an open-source, cross-platform system and provides an extensive suite of software tools for image analysis. National Library of Medicine sponsors ITK as a tool to support the Visible Human Project. ITK has become popular among developers that are interested in image processing projects. ITK provides extensive set of image processing methods for researchers. ITK does not provide visualization function of the result set. Therefore, a 3D visualization method is necessary for a complete medical solution.

Several algorithms and techniques have been developed for image segmentation. In this study, region-growing approach was chosen to determine the segments of the aorta. Region growing is classified as a pixel-based image segmentation method since it involves the selection of initial seed points. Region growing segmentation method takes a set of seeds and intensity interval as input along with the image and the regions are iteratively grown by comparing all unallocated neighboring pixels to the regions. Insight Toolkit's (ITK) region growing segmentation library is embedded into AMET to extract the aortic regions (Stewart, & et al, 2002).

Hounsfield Unit values of the pixels selected on CT slice are considered during region growing segmentation process. Segmentation is performed via user provided seed points and upper/lower threshold values. Threshold values that have been used to detect aorta pattern in a DICOM slice, are expressed in Hounsfield Units.

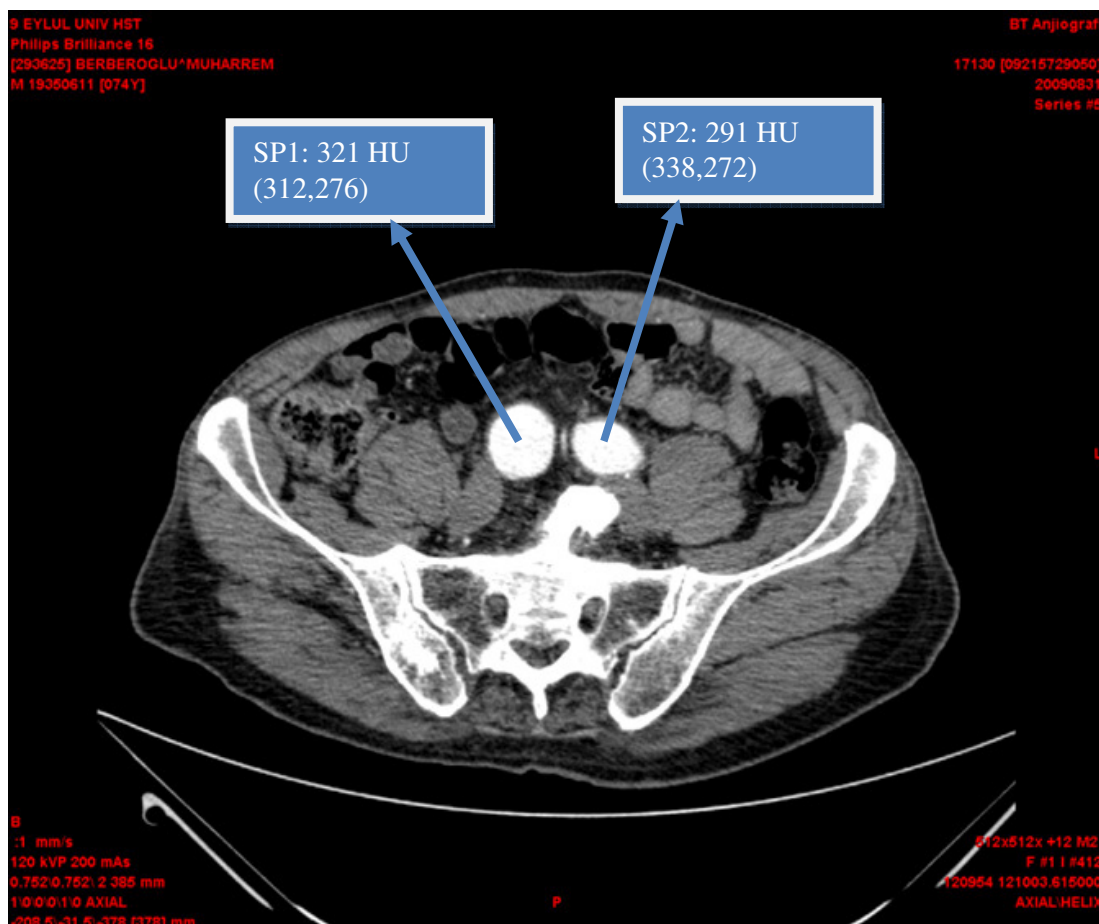


Figure 5.2 Reference Points and Hounsfield Unit threshold values are determined by physicians

DICOM Image Viewer Module provides interactive tools to display the Hounsfield Unit values of the point that resides on current mouse position on the selected DICOM slice. In figure 5.2, Hounsfield values and pixel coordinates of the selected two seed points are displayed. According to Hounsfield values of the aorta regions, physicians should define upper/lower threshold values.

For a successful segmentation, the seed points should be selected inside aorta region. After defining seed pixel, segmentation process is applied with appropriate Hounsfield Unit (HU) interval values. Our experiences showed that values ranging from 250 to 400 HU were suitable to view the effect of injected liquid in our dataset. Figure 5.3 represents the segmented images after segmentation of the aorta.

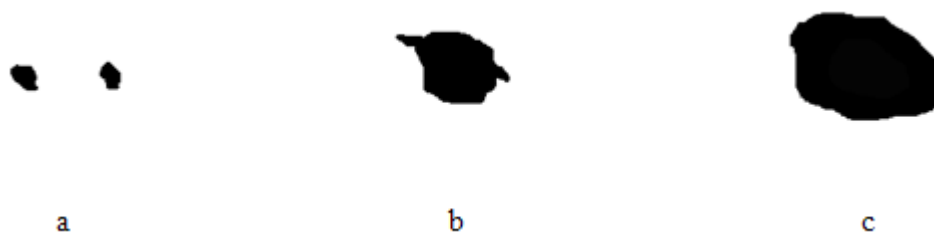


Figure 5.3 Segmented images a)Bifurcation case b)Renal Arteries c)Aneurysm region (aorta bulged)

Axial CT images are used and each image is segmented separately starting from lower part to upper part of the aorta. The “initial” slice is selected using “DICOM Viewer Module”. Segmentation is performed using seed points starting from initial image. To generate a whole aorta model, a slice, which corresponds to iliac arteries, should be selected. After initial slice is segmented, seed points for the next slice are generated automatically and there is no need to provide seed points for other slices.

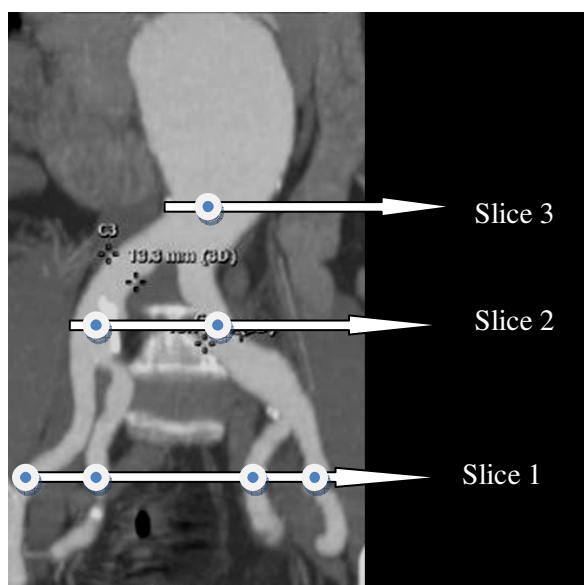


Figure 5.4 Initial slice selection for segmentation

The resulting set of segmentation includes the aorta regions for each image. An image may contain more than one aortic region. AMET provides visualization of the iliac arteries. If iliac arteries are requested in the 3D model, a seed point should be provided for each of them. For example, to generate the dataset for an aorta model that includes two iliac arteries, two seed points should be provided.

In Figure 5.4, three different initial slice alternatives are displayed. When the segmentation process is initialized from selected slice and all upper slices are segmented. The number of seed points required for each initial slice alternative is listed as follows:

- Slice 1: Four seed points should be provided for each bifurcation branch. Segmentation process continues separately for each seed point on the current slice until the branches are joined. When the branches are joined, two separate seed points become a single seed point.
- Slice 2: Two seed points should be provided for each iliac arteries. Since lower part is not be segmented, only iliac arteries with two branches and aneurysm area are generated.
- Slice 3: One seed point is adequate to generate the aorta aneurysm model. Iliac arteries and bifurcation will not be included in the model.

Physicians provide seed points for the initial slice and seed points for the other slices are generated automatically using the “center of gravity point” of the segmented region. Center of gravity (also known as centroid) of the segmented regions is also important to generate Aortic Center Line Path (ACLP).

5.1.2.1 Extraction Of Aorta Boundary

The segmented regions are processed in order to identify the boundary of the aorta in terms of pixel coordinates. To determine the boundary of the convex closed regions, edge detection is applied. Since the aim is to mark the pixels of the boundary and structure is in convex closed region format, the images are converted to monochrome, which includes only black and white. In monochrome image, white pixels correspond to aorta region and an edge is defined as an intensity discontinuity in the gray level. A pixel, which resides on the perimeter of the aorta region is obtained through intensity discontinuity. Using this discontinuity as a reference, all 8-neighbor pixels are scanned in clockwise direction. If a pixel is on the perimeter, it becomes the new reference and process continues until the first pixel is reached. This process continues until first pixel is reached again.

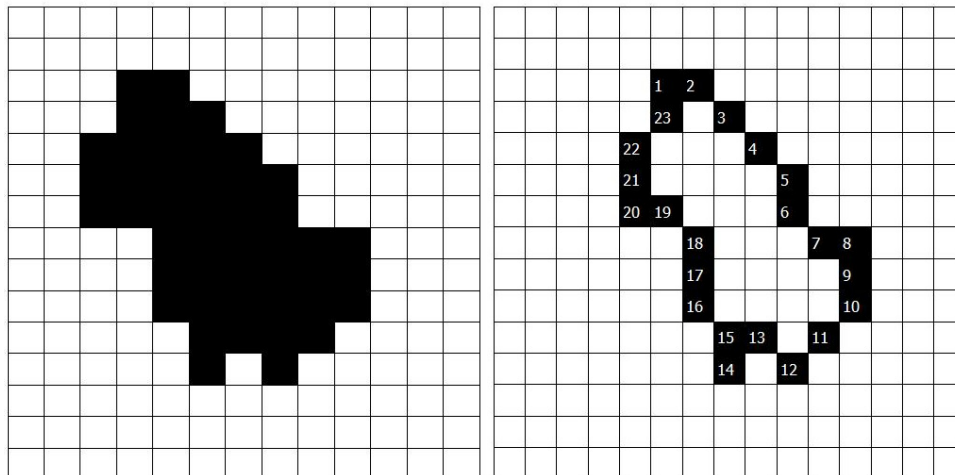


Figure 5.5 Outer boundary values are extracted by edge detection

A degraded edge detection process is depicted in figure 5.5. The edges are visited with clock-wise approach. The edge detection mechanism is listed as follows:

- A pixel is determined where an intensity discontinuity is detected. This pixel is set as the “current pixel”. These detected pixel coordinates are stored.
- There are eight different neighbors (up, up-right, right, down-right, down, down-left, left, up-left) of the current pixel. Scan direction is set to up direction. The pixel that is located in the scan direction is controlled if there is an intensity discontinuity.
- If the pixel has an intensity discontinuity, this pixel is set as current pixel and the process starts with first step for new pixel. If pixel does not qualify, scan direction is updated.
- When first pixel is reached, all boundary pixels are visited and stored for a single segmented region.

Edge Detection process creates a set of points which corresponds to boundary values of the aorta region in slice. All boundary values for all slices are calculated in same manner. While aorta has many branches in each slice, there may be more than one convex closed region. Boundary values for each convex closed region are stored separately in a tree data structure. In figure 5.6, relationship between slice boundary

values is depicted as a tree structure. “Regions 1” contains all boundary values of the slices that are located between thoracic aorta and the bifurcation area where aorta splits into two iliac arteries. “Regions 1.1” and “Regions 1.2” corresponds to first and second iliac arteries respectively and contain boundary values of the slices that are located in this interval. “Regions 1.1.1” and “Regions 1.1.2” correspond to further bifurcation of first iliac and the others correspond to second iliac.

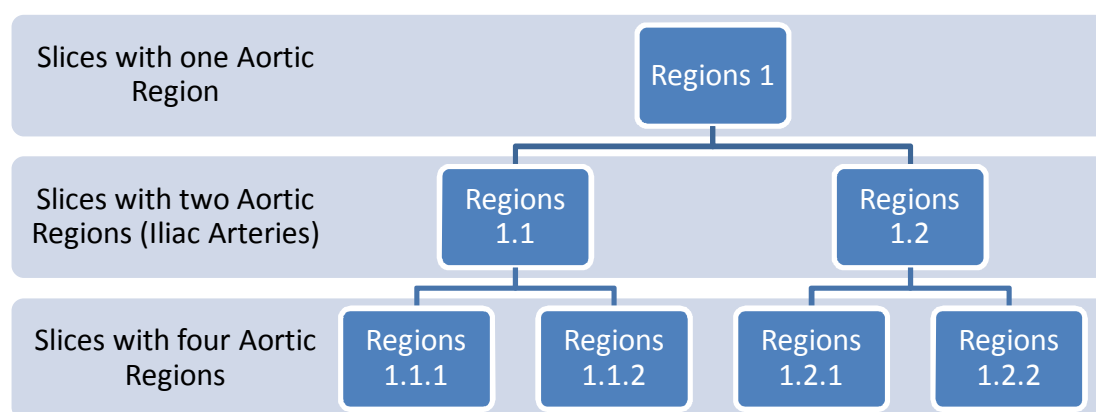


Figure 5.6 Tree structure of the boundary values

Generally, the most convenient method for expressing locations in an image is to use pixel coordinates. In the coordinate system, the image is treated as a grid of discrete elements, ordered from top to bottom and left to right. Pixel coordinates are integer values and range between one and the length of the row or column. Boundary values are stored as pixel coordinates (r, c, s) list for each region in the slices. In the representation, r denotes rows, c denotes columns and s denotes slice numbers. In Figure 5.7, three sample pixel coordinates for different slices are depicted.

A set of pixel coordinates are determined for each slice. The number of pixel coordinates in the set depends on the resolution of the DICOM image and area of the aortic region that resides on the slice. Pixel coordinates' set size is bigger in the slice where the aneurysm is the largest.

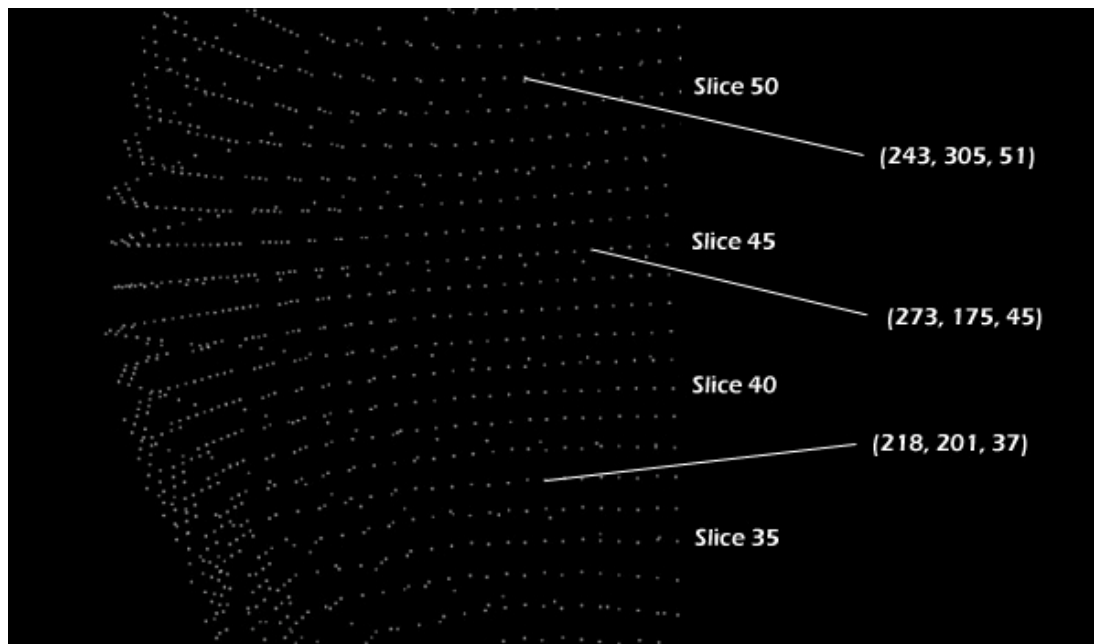


Figure 5.7 Pixel coordinates of boundary values

5.1.2.2 Aortic Center Line Path

AMET is a treatment-planning tool for aorta aneurysms, which provides aortic feature measurement capability on a 3D model of the aorta. Mathematical model generated from boundary values is used as a base data in 3D Visualization & Observation Module. Once the model is created, several measurements can be gathered on 3D aorta model with an interactive interface. As mentioned earlier, measurements are so critical to determine the method of the treatment (location of stent, type of stent, size of stent etc.).

Anatomical criteria used to predict the type and size of the graft were explained in earlier sections. The length of the proximal neck, diameter of the proximal neck, supra-renal angle, infra-renal angle, aneurysm length and length of each iliac segment are the most critical measurement values. These measurements are crucial in endovascular stent repair planning. According to these criteria, exact length, diameter and angle measurement values should be provided to the physicians.

The most obvious way to calculate a length (distance) in space is to use the Euclidean distance between two points. The distance between two points is the length of the path connecting them. In Euclidean three-space, the distance between

points (x_1, y_1, z_1) and (x_2, y_2, z_2) is $d = \sqrt{(x_2 - x_1)^2 + (y_2 - y_1)^2 + (z_2 - z_1)^2}$. However, this approach is not appropriate to measure curved structures. In figure 5.8, a curved line is illustrated. There are two alternatives to measure the distance between two points on the line. Left part of the figure 5.8 shows the Euclidean distance method where curve in the line is ignored. Conversely, right part of the figure 5.8 shows the curvature distance approach where curve is considered. Curvature distance result is either bigger than or equal to Euclidean distance result on a curved line.

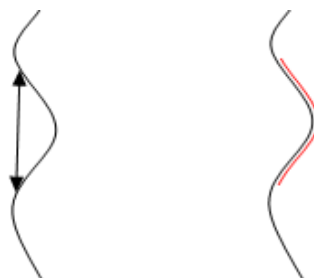


Figure 5.8 Euclidean distance versus curvature distance

Aorta has a curved structure and measurements may not be performed in linear approach. The curvature of the aorta may be not only in two-dimensional but also in three-dimensional where length calculation becomes more complex.

The Aorta Center Line Path (ACLP) is the most impressive part of the model, which makes angle calculation and length measurement more convenient in aneurysm diagnosis and evaluation. The exact length through the aorta is determined by using center line path. Center Line Path is generated from centroids of the segmented regions. Segmented aorta region is handled as a closed polygon to determine the centroid.

The problem of determining the area of a polygon seems complex but the final formula is particularly simple. Consider a polygon made up of line segments between N vertices (x_i, y_i) , $i = 0$ to $N-1$. The last vertex (x_N, y_N) is assumed to be the same as the first, i.e. the polygon is closed (Figure 5.9).

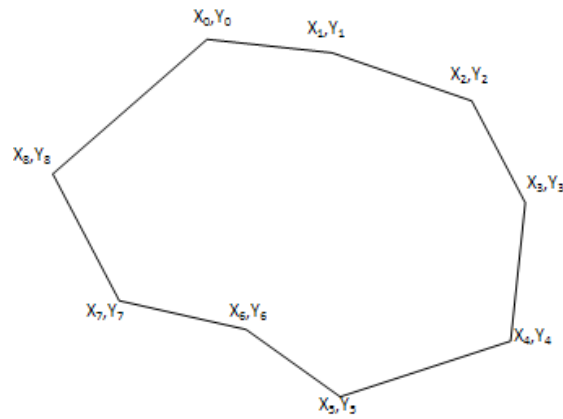


Figure 5.9: A polygon with 9 points

The area is given by;

$$A = \frac{1}{2} \sum_{i=0}^{N-1} (x_i y_{i+1} - x_{i+1} y_i) \quad (1)$$

The centroid is also known as the "centre of gravity" or the "center of mass". The position of the centroid assuming the polygon to be made of a material of uniform density is given below. As in the calculation of the area above, x_N is assumed to be x_0 , in other words the polygon is closed.

$$c_x = \frac{1}{6A} \sum_{i=0}^{N-1} (x_i + x_{i+1}) (x_i y_{i+1} - x_{i+1} y_i) \quad (2)$$

$$c_y = \frac{1}{6A} \sum_{i=0}^{N-1} (y_i + y_{i+1}) (x_i y_{i+1} - x_{i+1} y_i) \quad (3)$$

Centroid of the aorta is obtained by using the equation 2 and 3. Consecutive centroids are then connected to each other to form the aorta center line path (Figure 5.10).

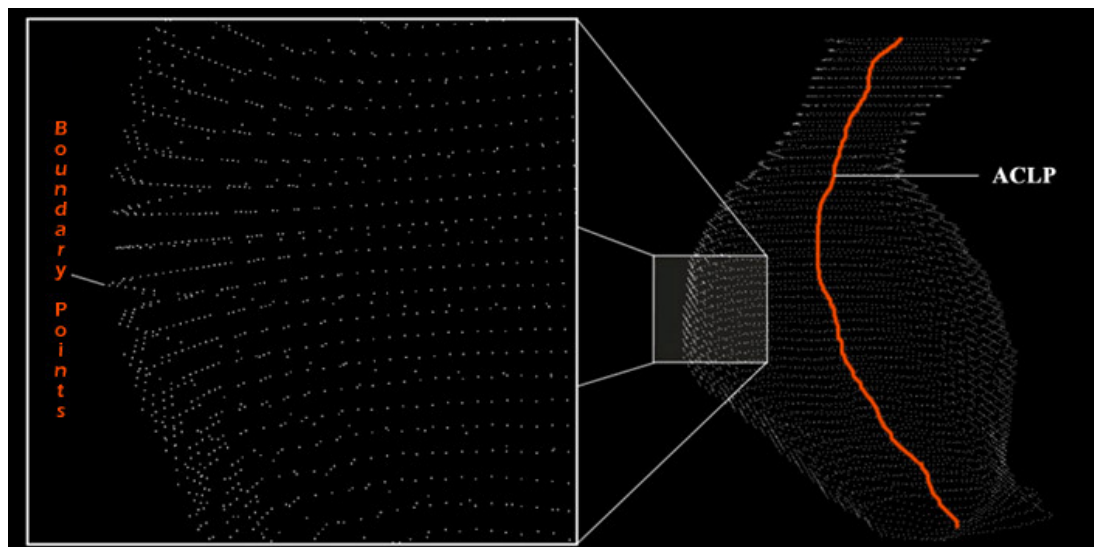


Figure 5.10 Boundary points of the aorta model and ACLP

Aortic segmentation module provides boundary values and aortic center line path for 3D visualization module. Boundary values are used to generate a three dimensional model of the aorta with surface construction methods that are explained in previous chapters. Aortic center line path is used to determine the length and angle values which are important for stent graft planning.

5.1.3 3D Visualization & Observation

3D Visualization and Observation module generates outer surface polygons using generated dataset (boundary values and aortic center line path) in segmentation module. Subsequent to segmentation and edge detection steps, all data is stored in a database. This avoids re-processing of the DICOM images and segmentation process. Database includes boundary values and centroid as pixel coordinates of the segmented region for each slice.

Smooth geometrical objects can be expressed with certain mathematical functions. For instance; ellipse, sphere shapes etc. If the surface has irregular geometry, it cannot be expressed with certain functions. Instead, irregular surfaces can be identified by using small surface components. Surface construction algorithms were used to generate polygons from slice outer edge coordinates.

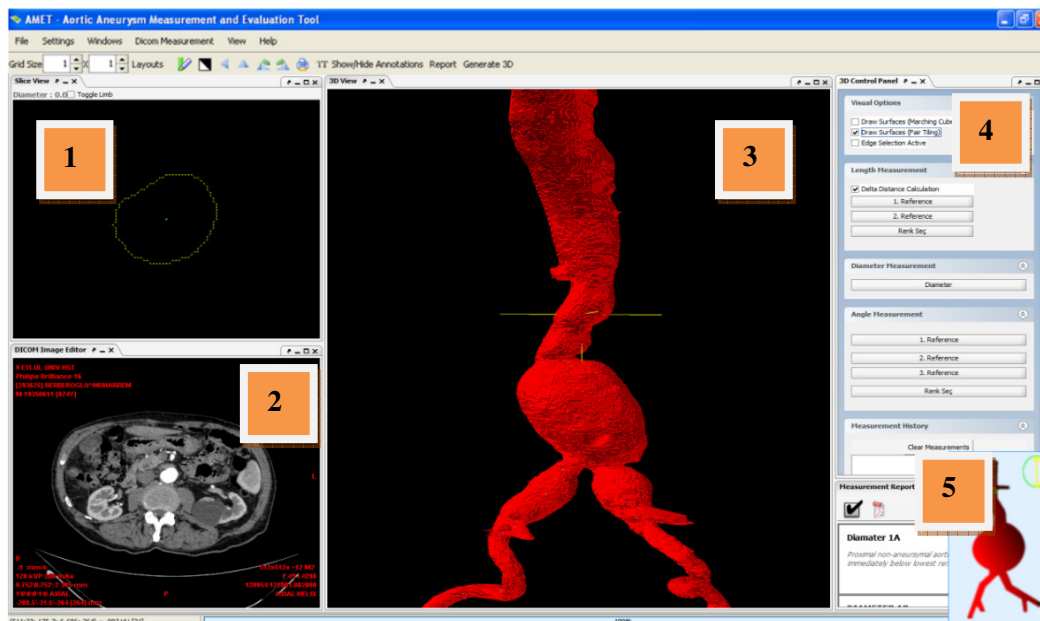


Figure 5.11 AMET (1) Image Viewer (2) DICOM Image Editor (3) 3D View Panel (4) Measurement Panel (5) Measurement Report

3D Aorta model was developed with Java OpenGL (jogl). OpenGL (Open Graphics Library) is a standard specification defining a cross-language, cross-platform API (Application Programming Interface) for building applications that produce 2D and 3D computer graphics. This module provides interactive aneurysm visualization and observation platform for physicians including pan, zoom, and rotate capabilities (Figure 5.11).

5.1.4 Measurement and Evaluation

Previous module generates an aorta model for physicians allowing them to analyze aneurysm in 3D perspective. However, several anatomical measurements are necessary for pre-procedural evaluation of endovascular abdominal aneurysm repair. Commonly used anatomical criteria to select the type of the graft can be summarized as follows (Stanley & et al. 2001):

- ✓ Length of the aortic neck
- ✓ Aortic neck diameter
- ✓ Supra-renal and infra-renal angle (neck angulation)
- ✓ Between the lowermost renal artery and the aortic bifurcation length
- ✓ Length of each iliac segment

- ✓ Diameter of each iliac segment

3D aorta model allows physicians to gather these measurements through measurement and evaluation module. Module provides an interface to make measurements by selecting necessary points on the model. Although all measurements are in control of the user, some key features are calculated automatically from intended vessel cross-section such as largest diameter. To determine the actual vessel length, curvature length calculation approach was developed over the ACLP. Curvature length is calculated via center points on the ACLP between two selected points by adding distance between consecutive center points. Curvature measurement generates more accurate results compared to Euclidean distance measurement in curved structures (Figure 5.12).

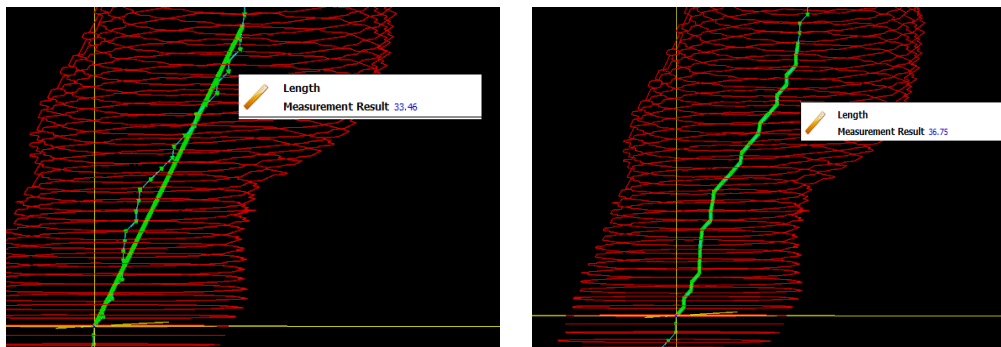


Figure 5.12 Euclidean Measurement and Curvature Measurement

Using ACLP approach, angles are also calculated over middle path. ACLP is an imaginary middle path that passes inside the curved structure of the aorta. Three points are selected on ACLP to determine the angle of a specific portion of the aorta. If $A(x_1, y_1, z_1)$, $B(x_2, y_2, z_2)$ and $C(x_3, y_3, z_3)$ are considered as three points in space, two intersecting lines (AB and BC) are formed. Aortic neck angulations are calculated using following formulation:

$$\vec{BA} \cdot \vec{BC} = |\vec{BA}| \cdot |\vec{BC}| \cdot \cos(\alpha) \quad (4)$$

$$\vec{BA} \cdot \vec{BC} = (x_1 - x_2)(x_3 - x_2) + (y_1 - y_2)(y_3 - y_2) + (z_1 - z_2)(z_3 - z_2) \quad (5)$$

$$|\vec{BA}| = \sqrt{(x_1 - x_2)^2 + (y_1 - y_2)^2 + (z_1 - z_2)^2} \quad (6)$$

$$|\vec{BC}| = \sqrt{(x_3 - x_2)^2 + (y_3 - y_2)^2 + (z_3 - z_2)^2} \quad (7)$$

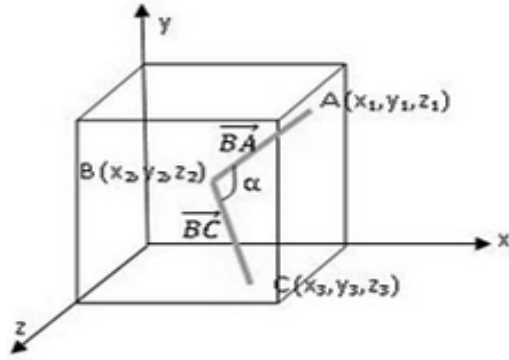


Figure 5.13 Angle calculation in 3D environment

If formulation “4” is regenerated, “ α ” angle value (angle between two lines in three-dimensional space) is obtained.

$$\alpha = \text{Arc cos}\left(\frac{\vec{BA} \cdot \vec{BC}}{|\vec{BA}| \cdot |\vec{BC}|}\right) \quad (8)$$

In summary, three different options are provided in AMET; “length measurement”, “diameter measurement” and “angle measurement”. To obtain length of a desired part two reference points on ACLP should be selected. On the other hand, three reference points residing on the ACLP are necessary for infra-renal and supra-renal angle measurement. Diameter of the aorta is calculated by either using “length measurement” option or “diameter measurement” option.

In this study, the aneurysm length, the proximal neck diameter, the proximal neck length, the alpha angle and the beta angle were evaluated. However, in AMET, physicians may define new length, diameter and angle representations. AMET has a flexible interface allowing new measurement quantities such as iliac diameter, iliac length and iliac bifurcation angle. In figure 5.14, measurement process is depicted for all quantities used in this study for a patient having abdominal aneurysm.

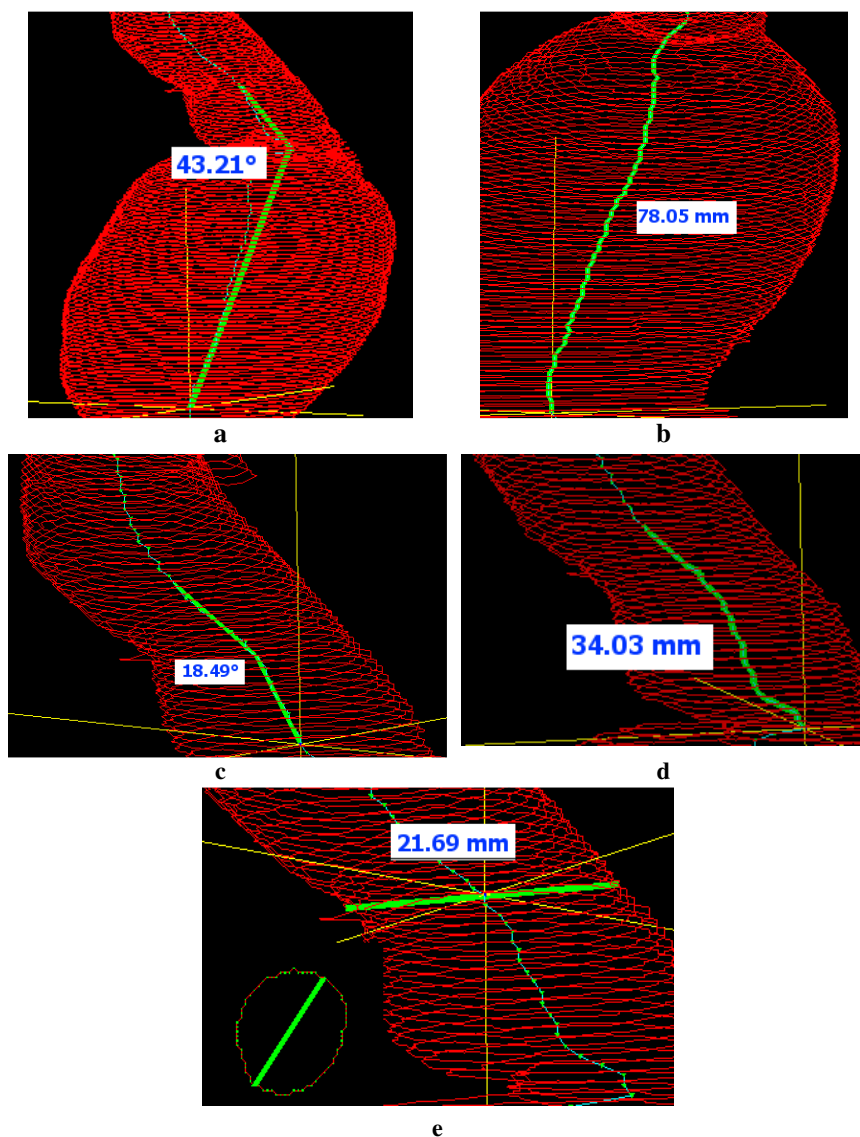


Figure 5.14 Measurements in AMET (a) Supra-renal angle (b) Aneurysm length of the AAA (c) Infra-renal angle (d) Proximal neck length of the AAA (e) Neck diameter

5.1.5 Stent Graft Selection

A stent graft is a tubular device, which is composed of special fabric supported by a rigid structure, usually metal as seen in figure 5.15. Each stent graft company has a series of different stent types. These stent types differ in size, quality and material.



Figure 5.15 Various stent types

Since anatomical features of the aneurysm are calculated by aorta visualization and evaluation tool, any stent selection method can be easily integrated to system. Traditionally, stent graft companies publish forms to get the information about the aneurysm and manually decide which stent is suitable for the aneurysm. If this manual mechanism can also be expressed in terms of an algorithm, AMET will be able to display the suggested stent type. This depends on the companies' stent inventory and stent selection criteria.

In figure 5.16, a sample stent device planning and sizing worksheet is displayed. The form includes fields for anatomical measurements. Physicians fill in the form with patients' anatomical measurements and send it to stent-supplier company. Stent graft experts process the filled form and appropriate stent alternatives are suggested to physicians.



ALL information must be complete:

Date: _____ Patient ID: _____

Hospital: _____

Physician Name: _____

Physician Signature: _____

Physician Phone #: _____

Physician E-mail: _____

DEVICE PLANNING AND SIZING WORKSHEET

Select Side of Main Body Introduction and Fixation Sites

Right iliac Left iliac

External Iliac (E) measurement _____ mm
(Minimum diameter; Inner wall to inner wall, from introduction site to aorta.)

Anatomical Measurements

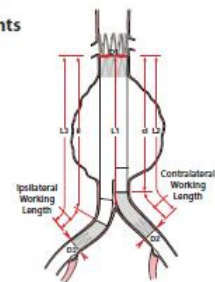
CT table position at:

_____ lowest renal artery
15 mm below lowest renal artery, check for 10% increase

_____ aortic bifurcation

_____ origin cl internal iliac

_____ origin il internal iliac



• When using CT for length, approximate lateral deviation/tortuosity and add to difference in table position.

Diameter: D1 D2 D3

Contralateral Iliac Leg

- From D2, select graft diameter.
- Using L2 and d1 length, complete the following equation.

minus=

L2 d1 Length Contralateral Working Length

- If choice of graft diameter or graft length is affected by other considerations, adjust accordingly.
- 8 and 10 mm graft diameters are also available.

Contralateral Leg (TFLE) Graft Diameters

D2 mm	Graft Diameter mm
10-11	12
12-13	14
14-15	16
16-17	18
18	20
19	22
20	24

Contralateral Leg (TFLE) Graft Lengths (mm)

Contralateral Working Length mm	Graft Length mm	Recommended Overlap stents
27-43	39*	1-1.5
44-60	56	1-1.5
61-77	73	1-1.5
78-94	90	1-1.5
95-111	107**	1-1.5
112-128	124**	1-1.5

*Assure adequate distal fixation lengths.
**Graft lengths 107 and 124 mm are available in 12 and 14 mm diameters only.

Figure 5.16 Stent Device Planning And Sizing Worksheet Sample (Image Courtesy, COOK Medical)

As mentioned earlier, there are common criteria to select a stent graft independent of the stent graft company. All these criteria are generated by developed aorta visualization and evaluation tool.

5.2 Web Based Aorta Visualization & Evaluation

Recent web-based technologies have created completely new possibilities to various medical information systems. Nevertheless, transferring 3D patient models through usual low bandwidth networks is difficult because of their large data size (Wakita, Hayashi, Kanai, Chiyokura, 2001). Medical data is usually very huge and transferring large amount of data over internet via browsers seems to be very rough. Still, there is no efficient way to share 3D medical information and applications to address this problem, some researchers are trying to develop web-based 3D medical systems.

5.2.1 Medical Data and Internet

Several sources distribute CT and MRI data on the Internet and offers opportunities for the use of medical images through the Internet. Using CT and MRI images, many research institutions have developed medical information systems. However, these information systems only allow these data are processed in standalone applications. Due to large amount of data, it is still difficult to segment images, build 3D applications on a web browser. To visualize an aneurysm nearly 300 DICOM images are used. This corresponds to an approximate size of 250 megabytes. A method of representing medical 3D models with small data size is an absolute requirement for realizing interactive and practical systems.

5.2.2 3D Web Technologies

Both hardware and software support for displaying realistic 3D graphics is growing every day. Therefore, there exist many technologies, which enable to present 3D data on the internet. The most popular 3D web standards are VRML, X3D, O3D and WebGL. All standards have advantages and disadvantages according to usage and capability (Turoňová, 2009).

VRML (Virtual Reality Modeling Language) is a standard file format for representing 3D interactive vector graphics, designed particularly with the World Wide Web in mind. VRML is a text file format where, e.g., vertices and edges for a 3D polygon can be specified along with the surface color, UV mapped textures, shininess, and transparency. VRML is a multiplatform format and accepted as a an international standard. It was designed especially for representing 3D content on the internet.

X3D is the ISO standard XML-based file format for representing 3D computer graphics, the successor to the Virtual Reality Modeling Language (VRML). WebGL is a context of the canvas HTML element that provides a 3D graphics API implemented in a web browser without the use of plug-ins. WebGL is based on OpenGL ES 2.0 and provides a programmatic interface for 3D graphics. O3D is an open source JavaScript API created by Google for creating interactive 3D graphics

applications that run in a web browser window. O3D is currently in Google's incubation lab, and is deployed as an experimental web browser plug-in.

5.2.3 AortaWeb : An AMET extension

As mentioned earlier, AMET was developed to visualize and diagnose abdominal aortic aneurysms. Although AMET is a platform-independent application, it still should be installed. Internet became a part of our life with growing bandwidth capabilities. Therefore, many applications are served over internet. The internet opportunities are the motivation behind AortaWeb. AortaWeb is an AMET web extension to display aorta models on internet via browsers (Figure 5.17).



Figure 5.17: AortaWeb

Generated 3D model data size is much less than the raw data. The images are already segmented and polygons are constructed in standalone AMET application. VRML is selected for visualization framework in AortaWeb due to support capabilities. The generated model can be easily ported to successor X3D format. Polygons gathered from AMET application is used to construct the 3D Model on a web page.

AortaWeb provides following features for visualization and evaluation of abdominal aortic aneurysms:

- ✓ Archiving mechanism of patients' aorta data
- ✓ Generation of pre-operation and post-operation visualizations
- ✓ Navigation over 3D model (pan, zoom, move)
- ✓ Displaying inner structure of the aorta

In medical imaging, Electronic Picture Archiving and Communication Systems (PACS) have been developed to provide storage, retrieval of images, access to images acquired with multiple modalities, and simultaneous access at multiple sites (Choplin, 1992). Once the images are retrieved from PACS, they are stored in terms of DICOM files. It is hard to organize patient data if connection to PACS does not exist and mobility is a necessity. Processed data is much smaller in terms of file size. In AortaWeb, processed data contains the aorta boundary polygon data and gathered measurements from AMET.

As well as CT data is scanned before EVAR process, there is also a CT scan after EVAR for follow-up purposes. Both CT scans may be processed by AMET and data transferred to AortaWeb. Using benefit of the web technology, AortaWeb has capability to display before-after visualization of the aneurysm. This is useful to see the results of the EVAR procedure.

CHAPTER SIX

CASE STUDY

In order to verify the accuracy, reliability, consistency, and repeatability of the AMET, data from randomly selected patients (obtained from D.E.U Medical Department) are used as test data set. The measurements were made in accordance with the anatomical criteria used by the physicians. Manual method corresponds to currently used method in radio diagnostic department. The aneurysm length, the proximal neck diameter, the proximal neck length, the alpha angle, and the beta angle were selected depending on these criteria.

6.1 Patient Dataset

Endovascular stent graft repair became widespread in Interventional Radiology Department, University of Dokuz Eylul in last decade. Data obtained from 33 patients treated with EVAR by the Interventional Radiology Department, University of Dokuz Eylul from January 2005 to March 2010, were analyzed retrospectively. Patients were all men with a mean age of 76 (age range: 60 – 84)

Multidetector CT examinations were performed by using a four-detector row scanner (Philips Medical Systems MX8000, the Netherlands). One hundred milliliters (300 mg of iodine per milliliter) of a non-ionic intravenous contrast material was administered, through a 20-gauge catheter inserted into an antecubital vein, at a rate of 4 mL/sec by using a power injector. Arterial phase imaging was performed by using bolus tracking. CT parameters were set at 120 kVp and 180 mAs and a 1.00-mm detector configuration was used. Three-millimeter-thick sections were reconstructed and downloaded to the picture archiving and communication system.

6.2 Measurement Methods

To determine the accuracy, reliability, consistency, and repeatability of the AMET, measurement results were compared with manual method. Aortic anatomy

was acquired from preoperative CT scans and angiograms. CT is required preoperatively to define the arterial anatomy.

In manual method, three-dimensional reconstructions of MDCT images were prepared using multiplanar maximum intensity projections (View Forum 4.1 – PMS 1.1 MIMIT, Philips Medical Systems) and MPR reformatted images which provides the measurement in 2D over sagittal, coronal or axial images which are generated by post-processing software. Aortic diameter was assessed directly from digital CT scans displayed on a workstation. The diameter measurements were performed on the minor axis with digital calipers. Neck length, the presence of a neck bulge, or reverse taper neck was assessed from CT scans with confirmation as needed from the angiography. Preoperative arteriograms were obtained selectively for questionable access or neck anatomy. Predeployment angiography with a marked catheter was taken in anterior–posterior with approximately 15 degrees of cranial–caudal angulations before endovascular graft selection.

AMET uses previously downloaded DICOM directories for each patient. These DICOM directories were downloaded from Picture archiving and communication system (PACS) server. DICOM directory was loaded and segmentation parameters were determined. These parameters were:

- Initial slice (starting slice of the segmentation)
- Intensity Interval Values
- Pixel Coordinates (starting point of the region-growing segmentation)

According to these parameters, segmentation was performed over the slices to generate the aortic regions. Once aortic regions were generated, boundary values and aortic center line path was created. Next, three-dimensional model of the aorta was generated by Fair Tiling approach. Aortic diameter was assessed directly from axial view displayed in AMET using diameter tool. Length measurements were assessed by defining two points on the aortic center line path. Angle measurements were assessed by defining three points on the aortic center line path.

6.3 Measurement Evaluation

Two radiologists (10 years and 7 years of CT angiography experience) in consensus evaluated and verified the arterial phase data to perform post-processing studies. The aneurysm length, proximal neck length, proximal diameter, infra-renal angle and supra-renal angle were calculated for 33 patients with manual method. A few weeks later same calculations were performed with AMET. In order to decide which method is more consistent and repeatable, second measurements were performed for 13 patients selected randomly from the study dataset.

In order to verify the accuracy of the tool, measurements were carried out on 33 patients' medical data at different times by both manual method and the AMET. Table 6.1 illustrates the results of measurements carried out by specialists using the manual method and the AMET.

Tablo 6.1 AMET and Manual Method Measurement Results (for 33 patients)

#	Manual Method					AMET				
	Aneurysm Length	Proximal Neck Length	Proximal Neck Diameter	Infra-renal Angle	Supra-renal Angle	Aneurysm Length	Proximal Neck Length	Proximal Neck Diameter	Infra-renal Angle	Supra-renal Angle
1	132,9	31,5	23,4	17	29	118,24	20,9	30,38	15,1	27,49
2	123,9	51,6	22,5	38	38	144,98	61,74	23,88	31,18	43,13
3	121,6	44,5	22,5	35	20	124,05	46,44	22,31	28,31	28,39
4	99,4	32,8	18,7	12	16	127,48	18,71	18,8	18,69	20,34
5	125	28,8	25,1	28	35	141,61	33,39	26,77	46,23	36,41
6	148	46,7	28,6	22	54	157,93	48,58	27,3	31,33	50,91
7	97,5	46,1	22,3	4	29	129,11	29,67	20,97	13,37	30,19
8	129,4	64,7	21,8	1	26,4	127,53	25,05	22,39	5,9	16,35
9	125	54,7	21,1	32	22	143,49	35,66	20,88	27,05	27,38
10	145,1	50	16,5	33	58	169,99	40,91	17,8	37,12	71,36
11	100,4	26,7	21,2	21	23	109,7	31,95	22,83	14,34	29,56
12	109,4	45,3	20,4	4	16	113,67	49,85	18,93	4,05	15,57
13	123	50	23	25	34	142,69	23,49	22,58	34,4	39,07
14	130,9	28,9	18,3	50	45	121,1	33,59	18,4	48,29	40,43
15	154	18	17	20	12	159,48	26,26	20,4	22,62	28,35
16	141,2	44,4	25,8	33	89	144,29	31,52	21,98	35,45	67,97
17	154,9	16,9	22,9	38	49	152,38	24,74	32,67	20,67	54,9

18	140	46,3	22,1	6	51	170,94	31,14	22,92	15,71	44,79
19	185,8	7	22,8	9	16	123,83	18,74	23,95	16,6	19,45
20	108,1	28,5	18	22	18	119,68	30,34	19,66	19,05	34,01
21	97,9	14,7	20,1	19	29	129,25	15,83	20	25,14	44,41
22	120	40	16,8	17	30	106,97	18,19	18,86	21,7	34,9
23	113	39,7	18	4	27	120,32	43,12	18,46	5,79	29,07
24	142	36	21,8	56,6	94	166,28	38,6	21,81	52,97	88,58
25	160,6	52	20,4	20	40	147,6	54,76	19,91	25,72	35,27
26	145,1	41,5	21,5	56	40	161,27	20,25	21,18	37,36	54,23
27	115,7	41,9	23	37	53	126,44	34,93	30,43	33,53	63,76
28	175,7	64,7	21	20	47	131,44	43,56	25,14	22,01	48,83
29	144,4	61,2	22,6	57	82	149,43	70,09	27,18	49,5	75,85
30	103,4	43,2	21,8	13	17	132,36	48,99	20,65	15,04	24,05
31	124,5	36,5	16,8	13	32	137,97	38,07	17,59	8,44	32,47
32	93	7	20,3	25	34	115,57	9,36	22,5	28,39	50,38
33	177,7	42,5	28,2	20	33	134,15	27,2	29,24	24,08	29,86

Pearson correlation analysis and Paired Sample T - Test analysis were done for measurement results of manual method and AMET using SPSS 17.0 (for Windows, SPSS Inc., Chicago, USA). The Paired Samples T Test compares the means of two variables. It computes the difference between the two variables for each case, and tests to see if the average difference is significantly different from zero.

Paired sample t-test is a statistical technique that is used to compare two population means in the case of two samples that are correlated. Paired sample t-test is used in 'before-after' studies, or when the samples are the matched pairs, or the case is a control study. The "P-value" in paired sample t-test is a probability, with a value ranging from zero to one. The "P-value" is the estimated probability of rejecting the null hypothesis of a study question when that hypothesis is true. The null hypothesis is usually a hypothesis of "no difference" e.g. no difference between the samples. If "P-value" is less than the chosen significance level (Conventionally $P < 0.05$) then you reject the null hypothesis.

Correlation is a technique for investigating the relationship between two quantitative variables. Pearson's correlation coefficient (r-value) is a measure of the strength of the association between the two variables. The correlation is evaluated as shown in Table 6.2.

Table 6.2 Correlation Value Interpretation

Correlation Value	Interpretation
≤ 0.50	Low
0.51 to 0.69	Acceptable
0.70 to 0.89	High
≥ 0.90	Excellent

Correlation results for 33 patients were summarized in Table 6.3.

Table 6.3 T – Test Results for 33 patients

	Manual Method Mean \pm SD	AMET Mean \pm SD	r-value (Pearson Correlation)
Aneurysm Length	130.56 \pm 24.15	136.40 \pm 17.66	0.46
Proximal Neck Length	38.91 \pm 14.87	34.11 \pm 13.75	0.61
Proximal Diameter	21.40 \pm 2.96	22.68 \pm 3.96	0.72
Infra-renal Angle	24.47 \pm 15.45	25.30 \pm 12.76	0.87
Supra-renal Angle	37.53 \pm 20.47	40.53 \pm 17.79	0.91

Correlation results show that proximal diameter, the supra-renal angle, and the infra-renal angle measured using manual method and AMET are correlated in a certain degree. On the other hand, the correlation for the aneurysm length and the proximal neck length also exists with a lower degree.

When all results are concerned together, there is a correlation between two methods. In order to decide which method is more reliable, consistent and repeatable; a sub-group with 13 patients was chosen randomly from 33 patients. Sub-group was evaluated twice for both manual method and AMET. To avoid operator dependency second measurement was performed at different time. The evaluation was performed in four steps at different times. These steps are listed in Table 6.4.

Table 6.4 Measurement steps for subgroup (13 patients)

Measurement Type	Measurement Time
Manual Method 1 st Measurement	T_0
Manual Method 2 nd Measurement	$T_0 + 1$ week
AMET 1 st Measurement	$T_1 = T_0 + 3$ weeks
AMET 2 nd Measurement	$T_1 + 1$ week

Table 6.5 illustrates the results of measurements carried out by specialists using the manual method for first and second measurement.

Table 6.5 Manual Measurement Results (for 13 patients)

#	Manual Method 1st Measurement					Manual Method 2nd Measurement				
	Aneurysm Length	Proximal Neck Length	Proximal Neck Diameter	Infra-renal Angle	Supra-renal Angle	Aneurysm Length	Proximal Neck Length	Proximal Neck Diameter	Infra-renal Angle	Supra-renal Angle
1	160,6	52	20,4	20	40	160	51	18,5	24	32
2	97,9	14,7	20,1	19	29	123,2	21,3	18,6	3	29
3	154	18	17	20	12	149,9	20,7	19,4	13	10
4	175,7	64,7	21	20	47	175,3	77,1	18,2	20	40
5	124,5	36,5	16,8	13	32	130,4	51,5	16,8	15	21
6	141,2	44,4	25,8	33	89	125,8	50,2	22,9	32	86
7	177,7	42,5	28,2	20	33	173,2	56,4	22,3	18	32
8	113	39,7	18	4	27	116	45,6	14,9	4	22
9	100,4	26,7	21,2	21	23	111,3	31,9	21,6	21	21
10	144,4	61,2	22,6	57	82	187	102	17,9	54	75
11	115,7	41,9	23	37	53	113,9	43,9	21,1	35	45
12	125	54,7	21,1	32	22	114,9	65,5	20,9	37	17
13	121,6	44,5	22,5	35	20	133,4	57,7	21	22	21

Correlation and T-Test were applied to two measurement samples (1st Measurement and 2nd Measurement) in order to find the correlation and the differences. Table 6.6 illustrates these test results for the manual method.

Table 6.6 Manual measurements repeated for randomly selected 13 patients

	1 st Measurement Mean ± SD	2 nd Measurement Mean ± SD	P-value	r-value
Aneurysm Length	134.75±26.52	139.56±26.43	0.28	0.83
Proximal Neck Length	41.65±15.12	51.90±21.98	0.01	0.91
Proximal Diameter	21.36±3.23	19.54±2.32	0.01	0.74
Infra-renal Angle	25.46±13.27	22.92±13.98	0.16	0.90
Supra-renal Angle	39.15±23.40	34.69±22.51	<0.01	0.94

The paired samples correlation coefficient in the Table 6.6 verifies how the sample distribution is related with one another. The paired sample correlation results are in the acceptable level. However, according to T-Test results, the values for the proximal neck length, proximal diameter, and the alpha angle is much lower than 0.05. There is a significant difference between these measurement groups. The result shows that there is no consistency between first and second measurements obtained with manual method.

Table 6.7 illustrates the results of measurements carried out by specialists using AMET for first and second measurement.

Table 6.7 AMET Measurement Results (for 13 patients)

#	AMET 1 st Measurement					AMET 2 nd Measurement				
	Aneurysm Length	Proximal Neck Length	Proximal Neck Diameter	Infra-renal Angle	Supra-renal Angle	Aneurysm Length	Proximal Neck Length	Proximal Neck Diameter	Infra-renal Angle	Supra-renal Angle
1	147,6	54,76	19,91	25,72	35,27	141,43	59,17	19,87	24,96	39,91
2	129,25	15,83	20	25,14	44,41	132,66	15,26	18,44	30,02	49,14
3	159,48	26,26	20,4	22,62	28,35	155,11	21,89	22,08	29,12	33,5
4	131,44	43,56	25,14	22,01	48,83	131,44	51,2	22,2	15,34	47,05
5	137,97	38,07	17,59	8,44	32,47	131,97	38,07	18,46	13,31	36,05
6	144,29	31,52	21,98	35,45	67,97	144,55	35,36	24,62	32,69	71,64
7	134,15	27,2	29,24	24,08	29,86	139,62	30,61	27,88	27,86	45,77
8	120,32	43,12	18,46	5,79	29,07	116,29	42,86	18,46	3,78	25,22
9	109,7	31,95	22,83	14,34	29,56	108,7	26,02	23,24	23,34	32,86
10	149,43	70,09	27,18	49,5	75,85	147,05	69,49	25,99	47,54	74,67
11	126,44	34,93	30,43	33,53	63,76	123,98	25,55	28,76	29,7	55,65
12	143,49	35,66	20,88	27,05	27,38	141,73	42,15	24,37	28,04	33,29
13	124,05	46,44	22,31	28,31	28,39	124,35	50,11	22,31	22,41	26,97

The correlation and T-Test was applied to measurement values obtained via the AMET method with same approach. Table 6.8 illustrates these values. The paired sample correlation results are in the acceptable level with higher correlation values than manual method. According to the T-Test results, there is no significant

difference determined for all measurements. In other words, there is no meaningful difference for measurement groups (1st and 2nd measurement with AMET).

Table 6.8 Measurements repeated using AMET for randomly selected 13 patients

	1 st Measurement Mean ± SD	2 nd Measurement Mean ± SD	P-value	r-value
Aneurysm Length	135.20±13.62	133.76±13.01	0.15	0.97
Proximal Neck Length	38.41±13.77	39.05±15.60	0.65	0.95
Proximal Diameter	22.79±4.05	22.82±3.46	0.96	0.89
Infra-renal Angle	24.76±11.43	25.23±10.55	0.74	0.90
Supra-renal Angle	41.62±17.16	43.97±15.68	0.17	0.99

Both results show that AMET is more consistent and repeatable when compared with manual method. Reliability of two methods is also evaluated by using Cronbach's Alpha Model. Cronbach's is a coefficient of reliability. It is commonly used as a measure of the internal consistency or reliability. Table 6.9 illustrates Cronbach's Alpha results for the AMET and Manual Method. The results show that, the reliability values obtained for AMET are better than the manual method for all anatomical criteria.

Table 6.9 Reliability of manual method and AMET

Features	Cronbach's Alpha	
	AMET 1 st and 2 nd Measurements	Manual Method 1 st and 2 nd Measurements
Aneurysm Length	0.98	0.91
Proximal Neck Length	0.97	0.92
Proximal Diameter	0.94	0.82
Infra-renal Angle	0.95	0.95
Supra-renal Angle	~1.00	0.97

Table 6.10 illustrates the elapsed time to measure the aortic neck angles in manual method and AMET for 33 patients respectively. The elapsed time was measured

between the start of loading medical data and end of gathering aortic neck angles. The results showed that AMET outperforms manual method in terms of measurement time.

Table 6.10 Measurement time comparison between manual method and AMET

#	Manual Method	AMET
1	7' 25"	1' 50"
2	6' 50"	2' 02"
3	10' 18"	1' 52"
4	7' 45"	2' 03"
5	11' 10"	2' 04"
6	9' 45"	1' 18"
7	11' 50"	2' 15"
8	12' 35"	1' 44"
9	6' 42"	1' 52"
10	10' 43"	2'
11	9' 45"	2' 06"
12	6' 40"	1' 59"
13	5' 50"	2' 01"
14	7' 46"	2'
15	5' 35"	1' 57"
16	8' 30"	1' 47"
17	8' 57"	1' 50"
18	8' 25"	1' 59"
19	10' 2"	1' 52"
20	9' 1"	1' 48"
21	9' 55"	1' 49"
22	9' 50"	1' 57"
23	7' 24"	1' 43"
24	10' 20"	2' 06"
25	7' 55"	1' 45"
26	12'	1' 41"
27	5' 31"	1' 55"
28	7' 33"	1' 45"
29	8' 23"	1' 46"
30	9' 12"	2' 01"
31	8' 16"	1' 35"
32	7' 54"	1' 42"
33	6' 14"	1' 54"
Average	8' 40"	1' 52"

In manual method, physicians have to work on different cross-sectional images to get reliable measurements. Physicians try to locate the correct view of the MPR images for infra-renal and supra-renal angle calculation by drawing two straight lines in the middle of the aorta. Calculation process is not so complicated for infra-renal angle, because the angulation is not sharp in this region. However, aneurysm usually makes a sharp angulation at the beginning of the aneurysm where supra-renal

angulation exists. Manual method is not so successful at repeated supra-renal angle calculation. Our statistical results prove this situation ($p < 0.01$ for Supra-renal Angle and $p = 0.16$ for Infra-renal Angle, Table 6.6). On the other hand, in AMET, p values for angle measurements are bigger than 0.05.

Distance between the lowermost renal artery and the beginning of the aneurysm is measured for proximal neck length and orthogonal cross section of the neck is measured for the proximal diameter. However, in manual method, to locate the lowermost renal artery and beginning of the aneurysm is difficult using MPR images and they do not provide cross-section view. Proximal neck length and proximal diameter measurement results are inconsistent when the manual method is repeated. Statistical results prove this situation ($p = 0.01$ for proximal neck length and $p = 0.01$ for proximal diameter).

When we focus on the repeated measurement results of AMET, p values are bigger than 0.05. In addition, Cronbach's alpha (reliability) results prove that AMET more reliable than manual method when measurements are repeated. Physicians should make more measurements on the MPR images to determine the actual value of the criteria. Moreover, when measurement time is considered, method provided by AMET is faster than the manual method.

In brief, we performed several tests to evaluate the reliability and repeatability of the measurement methods that used in AMET. We compared the results obtained from AMET with the results of manual method. Manual method is a combination of several techniques that are considered as prosperous methods. The results of manual method are used to predict stent size and type. Determined stents are successfully applied to patients. To evaluate the reliability, we applied T-Test for manual method and AMET results. Correlation results show that aortic features using manual method and AMET are correlated.

A sub group of patients was randomly selected from 33 patients and aortic features of these patients were measured twice at different times both for manual method and AMET. Paired Samples T-Test showed that the correlation values are very high and no significance is determined for measurements in AMET. On the

other hand, correlation values for manual method was not high as AMET results. In addition, Cronbach's alpha results prove that AMET more reliable than manual method when measurements repeated.

CHAPTER SEVEN

CONCLUSIONS

Different image processing and several imaging modalities have accelerated three-dimensional modeling in medical area. Nowadays, 3D computer visualization and evaluation have played a major role in medical imaging and evaluation. The developed software solution Abdominal Aortic Measurement and Evaluation Tool (AMET) overcomes aneurysm measurement and evaluation problems during the stent selection process for Abdominal Aortic Aneurysm. Hardware needs and operating system independency properties are important features of the AMET. The application offers privatization opportunities and the study presents an aortic measurement and visualization application platform, which is specialized for physicians. In addition, the application provides a user-friendly interface and improved measurement capabilities.

The aim of this study is to model the aortic vein and to provide measurement capabilities on this model. These measurements help the physicians in the stent selection process. Therefore, the physicians can easily determine stent – graft type. AMET is a platform – independent package, and customized for the modeling and measurement of an aortic vessel.

In stent–graft repair, the importance of appropriate stent choice, the placement of the selected stent into the suitable location, and identification of possible complications after stent placement cannot be considered separately. Stent selection is a time consuming process in stent – graft repair. Moreover, monitoring of intravascular stent location before the operation affects the treatment results. Depending on the obtained results, it was proved that using AMET reduces time required for stent selection pre-process. Currently used methods in medical services, aortic neck angulation measurements are mostly manual; conventional methods of evaluation need repetition.

AMET is a complete computerized solution for abdominal aortic aneurysm diagnosis and stent graft planning. It provides a graphical user interface to load and

browse images acquired using Computed Tomography in DICOM format. AMET is able to generate a 3D model of the aorta and subsequently the aneurysm and is equipped with specialized tools to measure aortic features.

There is no specific hardware or operating system requirements, AMET run on any vendor's graphics card and on any operating that supports JAVA. CT scanner bundled 3D software is dependent on complex graphic workstations and does not allow data portability. For better 3D visualization, high performance graphic cards are recommended. Several Java libraries are used in the development of the modules. This brings operating system independency capability to AMET. AMET assists physicians to measure aortic features by ACLP approach before stent graft repair. ACLP is an important approach to calculate the measurements for the aorta accurately and to minimize variance in the determination of the aortic criteria. AMET presents a complete PC-based solution for abdominal aortic aneurysm diagnosis and stent graft planning.

In addition, a list of stent selection criteria is defined in AMET. Each measurement result is associated with an item in the list and a report is generated for stent graft planning. Most stent vendors request aortic measurements to predict stent type and size. AMET can be configured to generate vendor specific reports.

AMET has several limitations. Segmentation quality in AMET is affected by medical data deficiencies due to misuse of contrast media. Non-uniform spread of the contrast media causes inhomogeneous intensity through the aorta and improper segments may be generated. Spatial resolution of DICOM CT images affects the quality of constructed 3D model and ACLP. Smaller thickness values and high axial resolution generate a smoother ACLP and 3D model. Determination of the upper and lower threshold HU values are also key factors of a successful segmentation. Physicians determine threshold values and improper input may create empty or faulty segments. AMET uses 2D image processing techniques. Therefore, the relationship between segments should be handled to generate surface polygons of 3D model. An extra processing effort is required to generate this relationship. Fair Tiling method was created to overcome this disadvantage in surface polygon construction.

The accuracy and usability of the tool was tested with a series of measurements that are carried out on the selected patients' group. Obtained statistical results are evaluated and compared with manual method. Test results show that the AMET is more reliable, consistent, and repeatable.

AortaWeb, web extension of AMET, is a promising web based aneurysm evaluation tool. Physicians are able to visualize aorta and its' extents on a web browser and access patient data from anywhere in an organized way. It brings a high benefit for medical physicians by observing the development around the aneurysm after EVAR procedure.

In conclusion, AMET is a promising candidate to perform an important role for pre-procedural evaluation of EVAR and ACLP is an important method to calculate angulations, and the length of the aorta. Statistical analysis proved that angle and the length calculation by using ACLP provides more reliable, consistent, and repeatable results.

REFERENCES

- Aarts, N.J.M., & et al. (1999). Abdominal aortic aneurysm measurements for endovascular repair: intra-and interobserver variability of CT measurements, *European Journal of Vascular and Endovascular Surgery*, 18, 475 – 480.
- Abdominal Aortic Aneurysm*. (n.d.). Retrieved March 8, 2011, from http://www.medicinenet.com/abdominal_aortic_aneurysm/article.htm
- Al-Omran, M., Verma, S., Lindsay, T.F., Weisel, R.D., Sternbach, Y. (2004). Clinical decision making for endovascular repair of abdominal aortic aneurysm. *Circulation*, 110(23), e517-23.
- Albertini, J.N., & et al. (2000). Anatomical Risk Factors for Proximal Perigraft Endoleak and Graft Migration Following Endovascular Repair of Abdominal Aortic Aneurysms. *European Journal of Vascular & Endovascular Surgery*, 19, 308–312.
- Bertges, D. J., & et al. (2003). Abdominal aortic aneurysm size regression after endovascular repair is endograft dependent. *Journal of vascular surgery : official publication, the Society for Vascular Surgery and International Society for Cardiovascular Surgery, North American Chapter*, 37(4), 716-23.
- Blum, U., & et al. (1997). Endoluminal Stent–Grafts for Infrarenal Abdominal Aortic Aneurysms. *The New England Journal of Medicine*, 336(1), 13-20.
- Cao, P. & et al. (2002). Predictive factors and clinical consequences of proximal aortic neck dilatation in 230 patients undergoing abdominal aorta aneurysm repair with self-expandable stent-grafts. *Journal of Vascular Surgery*, 37, 1200-1205.
- Chaikof, E. L., & et al. (2002). Reporting standards for endovascular aortic aneurysm repair. *Journal of Vascular Surgery*, 35(5), 1048-1060.

Cheng, S.W. (2010). Endovascular Stent Graft for Aortic Diseases. *Graft*, 91-92.

Choke E., & et al. (2006). Outcomes of endovascular abdominal aortic aneurysm repair in patients with hostile neck anatomy. *CardioVascular and Interventional Radiology*, 29, 975-980.

Choplin, R., (1992).Picture archiving and communication systems: an overview, *Radiographics*, 12,127-129.

Chuter T.A.M., & et al. (1996). Clinical experience with a bifurcated endovascular graft for abdominal aortic aneurysm repair. *Journal of Vascular Surgery*, 24, 655–666.

Chervu, A., Clagett, G.P., Valentine, R.J., Myers, S.I., Rossi, P.J. (1995). Role of physical examination in detection of abdominal aortic aneurysms. *Surgery*, 117, 454-457

Clouse, W.D.,& et al. (1998). 3rd. Improved prognosis of thoracic aortic aneurysms: a population-based study. *JAMA*, 280, 1926–1929.

Dillavou, E. D., & et al.(2003). Does hostile neck anatomy preclude successful endovascular aortic aneurysm repair?. *Journal of Vascular Surgery*, 38(4), 657-663.

Dillon, M., Cardwell, C, Blair, P.H., Ellis, P., Kee, F., Harkin, D.W. (2007). Endovascular treatment for ruptured abdominal aortic aneurysm. *Cochrane Database of Systematic Reviews*, 1, CD005261.

Endovascular aneurysm repair. (July 2008). Retrieved March 8, 2011, from <http://radiopaedia.org/articles/endovascular-aneurysm-repair>

Endovascular Stent Graft. (January 2010). Retrieved March 8, 2011, from <http://www.vascularweb.org/vascularhealth/Pages/EndovascularStentGraft.aspx>

- Ernst, C.B. (1993). Abdominal Aortic Aneurysm, *The New England Journal of Medicine* 328(16),1167-1172.
- Filis, K.A., Arko, F.R., Rubin, G.D., Zarins, C.K.(2003) Three-dimensional CT evaluation for endovascular abdominal aortic aneurysm repair. Quantitative assessment of the infrarenal aortic neck. *Acta Chir. Belg* , 103,81-8
- Fleming C., & et al. (2005). Screening for abdominal aortic aneurysm: A best-evidence systematic review for the U.S. Preventive Services Task Force. *AHRQ Pub*, 05,0569.
- Gravereaux, E. C., & et al. (2001). Risk of spinal cord ischemia after endograft repair of thoracic aortic aneurysms. *Journal of vascular surgery : official publication, the Society for Vascular Surgery and International Society for Cardiovascular Surgery, North American Chapter*, 34(6), 997-1003.
- Ham, A.C., & et al. (2005). Two-Year Outcomes after Conventional or Endovascular Repair of Abdominal Aortic Aneurysms. *Society*, 20(2), 183-189.
- Haralick, R. M., Shapiro, L.G. (1985). Image segmentation techniques. *Computer Vision, Graphics, and Image Processing*, 29, 100-132
- Hovsepian, D.M. & et al.(2001). Endovascular abdominal aortic aneurysm repair in 144 patients: correlation of aneurysm size, proximal aortic neck length, and procedure-related complications, *Journal of Vascular Interventional Radiology*, 12, 1373–1382.
- Horowitz, S., & Pavlidis, T. (1974). Picture segmentation by a directed split and merge procedure. *In Proceedings of the 2nd International Joint Conference on Pattern Recognition*, 424 – 433.

- Interventional Radiologists Treat Abdominal Aneurysms Nonsurgically.* (n.d.). Retrieved March 8, 2010, from <http://www.sirweb.org/patients/abdominal-aortic-aneurysms>
- Kantonen, I., & et al. (1999). Mortality in ruptured abdominal aneurysms. *European Journal of Vascular and Endovascular Surgery*, 17, 208–212.
- König, A., Gröller, E., (January 2001). *3D Medical Visualization: Breaking the Limits of Diagnostics and Treatment.* August 2010, http://www.ercim.eu/publication/Ercim_News/enw44/koenig.html.
- Kunio, D., (2006). Diagnostic imaging over the last 50 years: research and development in medical imaging science and technology. *Physics in medicine and biology*, 51(13), 5-27.
- Lederle, F.A., Simel, D.L.(1999). Does This Patient Have Abdominal Aortic Aneurysm?, *The Rational Clinical Examination*, 281, 77-82.
- Lee A.,(Dec 2008). *X-ray, Ultrasound, Magnetic, and Nuclear Modalities.* August 2010, <http://www.suite101.com/content/types-of-medical-imaging-a85622>.
- Lee, W.A. (2010). Endovascular abdominal aortic aneurysm sizing and case planning using the TeraRecon Aquarius workstation. *Vascular and endovascular surgery*, 41(1), 61-7.
- Linninger, A.A., & et al. (2005). Mimics Image Reconstruction for Computer - Assisted Brain Analysis. *Imaging*, 1,12.
- Lorensen,W., Cline,E. (1987). Marching Cubes: A high resolution 3D surface construction algorithm. *Computer Graphics*, 21, 4

- Malina, M., & et al. (1997). Changing Aneurysmal Morphology After Endovascular Grafting: Relation to Leakage or Persistent Perfusion, *Journal of Endovascular Surgery*, 4, 23-30.
- Mandziak, D.M., Stanley, B.M., Foreman, R.K., Walsh, J.A., Burnett, J.R. (2004). Outcome of endoleak following endoluminal abdominal aortic aneurysm repair. *ANZ J Surg*, 74(12), 1039-42.
- Matsumura, J.S., Brewster, D.C., Makaroun, M.S., Naftel, D.C. (2003). A multicenter controlled clinical trial of open versus endovascular treatment of abdominal aortic aneurysm. *Journal of Vascular Surgery*, 37, 262-271.
- May, J., & et al. (1999). Adverse events after endoluminal repair of abdominal aortic aneurysms: A comparison during two successive periods of time. *Journal of Vascular Surgery*, 29, 32-39.
- Moore, H.D., & Sydney, M.B.,(1967). Diagnosis of Rupture of Abdominal Aortic Aneurysms. *The Lancet*, 290 (7508), 184-186.
- Mustra, M., Delac, K., Grgic, M.(2008) Overview of the DICOM standard. *ELMAR*, 39-44
- Parodi J.C., Palmaz J.C., Barone H.D.(1991) Transfemoral intraluminal graft implantation for abdominal aortic aneurysms. *Ann Vasc Surg*, 5, 491-499.
- Pearson's Product Moment Correlation Coefficient*. Retrieved March 8, 2011, from <http://www.acastat.com/Statbook/correlation.htm>
- Perler, B.A., & Becker, G.J. (1997). *Vascular Intervention: A Clinical Approach*. New York : Thieme Medical Publishers

- Pimenta, S.,Tavares, J.M.R.S., Jorge, R.N., Alexandre, F., Mascarenhas, T., El Sayed, R.F. (2006). Reconstruction of 3D Models from Medical Images: Application to Female Pelvic Organs. *CompIMAGE*, 8217,06.
- Resch, T. & et al. (2000). Midterm changes in aortic aneurysm morphology after endovascular repair. *Journal of Endovascular Therapy*, 7, 279-285.
- Resch, T., & et al. (1999). Abdominal aortic aneurysm morphology in candidates for endovascular repair evaluated with spiral computed tomography and digital subtraction angiography. *Journal of Endovascular Surgery*, 6, 227-32.
- Robbins, M., & et al. (2005). Comerota, Suprarenal Endograft Fixation Avoids Adverse Outcomes Associated with Aortic Neck Angulation, *Annals of Vascular Surgery*, 19, 172-177.
- Rockman, C.B., & et al. (2002).Aneurysm morphology as a predictor of endoleak following endovascular aortic aneurysm repair: do smaller aneurysm have better outcomes?. *Annals of Vascular Surgery*; 16, 644-651.
- Rödel, S.G., Geelkerken, R.H., Herwaarden, J.A., Kunst, E.E., van den Berg, J.C., van der Palen, J., Teijink, J.A., Moll, F.L. (2006). Consistency in endovascular aneurysm repair suitability assessment requires group decision audit. *J Vasc Surg*, 43(4),671-6.
- Sande, E., Martinsen,A., Hole, E., Olerud, H., (2010). Interphantom and interscanner variations for Hounsfield units-establishment of reference values for HU in a commercial QA phantom. *Physics in Medicine and Biology*,55,5123
- Shapiro, L., Stockman, G. (2001), *Computer Vision* (1st ed.).New Jersey:Prentice Hall

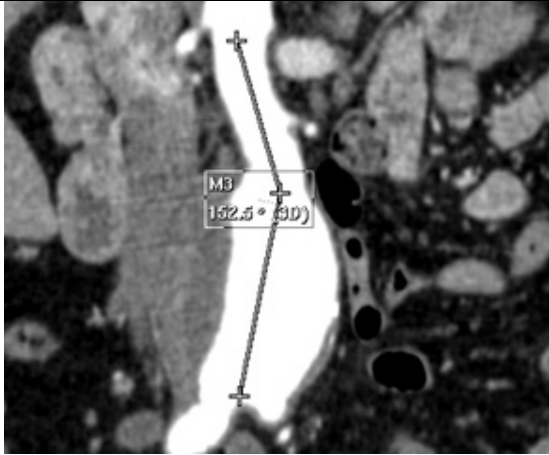
- Slater, B.J., Harris, E.J., & Lee, J.T. (2008). Anatomic Suitability of Ruptured Abdominal Aortic Aneurysms for Endovascular Repair. *Annals of Vascular Surgery*, 22, 716-722.
- Stanley, B.M., & et al. (2001). Evaluation of Patient Selection Guidelines for Endoluminal AAA Repair With the Zenith Stent-Graft : The Australasian Experience. *Journal of Endovascular Therapy*, 457-464.
- Sternbergh, W.C., Carter, G., York, J.W., Yoselevitz, M., & Money, S.R. (2002). Aortic neck angulation predicts adverse outcome with endovascular abdominal aortic aneurysm repair. *Journal of Vascular Surgery*, 35, 482-486.
- Stewart, R.D., Fermin, I., Opper, M. (2002). "Region growing with pulse-coupled neural networks: an alternative to seeded region growing", *IEEE transactions on neural networks*, 13(6), 1557-62.
- Stone, P.A., Hayes, J.D., Aburahma, A.F., et al.(2005). Ruptured abdominal aortic aneurysms: 15 years of continued experience in a southern West Virginia community. *Ann Vasc Surg*, 19, 851-857.
- Stytz, M.R., Frieder, G., & Frieder, O. (1991) Three-dimensional medical imaging: algorithms and computer systems. *ACM Computing Surveys (CSUR)*, 23(4), 421-499.
- Teufelsbauer, H., & et al. (2002). Endovascular stent grafting versus open surgical operation in patients with infrarenal aortic aneurysms. *Circulation*, 106, 782-787.
- Treiman, G. S., & Bernhard, V. M. (1998). Endovascular treatment of abdominal aortic aneurysms. *Annual review of medicine*, 49, 363-73.
- Turoňová, B.(2009). *3D Web Technologies And Their Usability for The Project 3D Mobile Internet*, Retrieved March 8, 2011, from http://www.rdc.cz/download/publications/Turonova_2009_3DWeb.pdf.

- Upchurch, R., & Criado, E. (2008). *Aortic Aneurysms: Pathogenesis and Treatment* (1st ed.). New Jersey:Humana Press.
- Utku, S., Baysal, H., Tosun, M., Kut, A. (2010). A new approach for surface construction in medical applications: Fair tiling. *BIYOMUT*,15,01.
- Waasdorp, E.J., & et al. (2005). Aneurysm Diameter and Proximal Aortic Neck Diameter Influence Clinical Outcome of Endovascular Abdominal Aortic Repair: A 4-Year EUROSTAR Experience. *Annals of Vascular Surgery*, 19, 755-761.
- Wakita,A.,Hayashi,T.,Kanai,T., Chiyokura,H.(2001).Using Lattice for Web-based Medical Applications,” *ACMWEB3D*, 29-34
- Wolf, I., & et al. (2005). The medical imaging interaction toolkit. *Medical image analysis*, 9(6), 594-604.
- Zarins, C.K. , & et al. (1999). AneuRx stent graft versus open surgical repair of abdominal aortic aneurysms: Multicenter prospective clinical trial. *Journal of Vascular Surgery*, 29,292-308.

APPENDICES

A. Measurement In Manual Method And AMET

In manual method, MPR images are used to obtain anatomical features of the aneurysm. In MPR, a volume is built by stacking the axial images and it provides a new viewpoint through the volume in a different plane. MPR allows images to be created from the original axial plane in either the coronal, sagittal, or oblique plane. The planes of human body are presented in Appendix C.

	Supra-renal angle
	Infra-renal angle

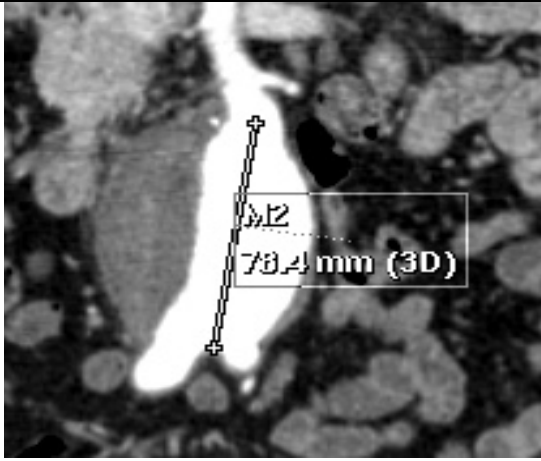
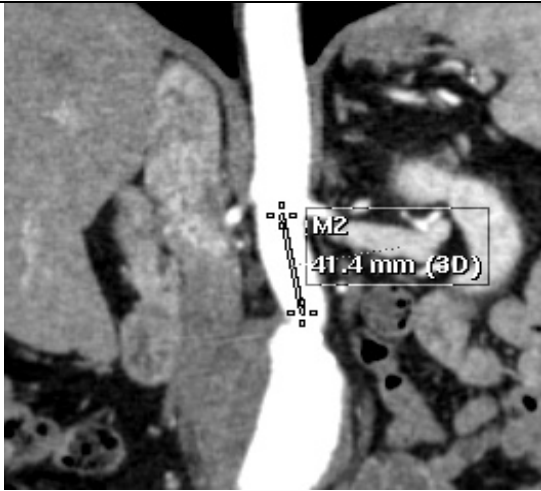
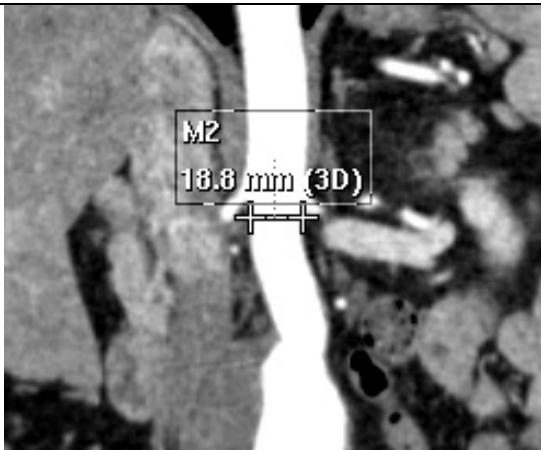
	Aneurysm length of the AAA
	Proximal neck length of the AAA
	Neck diameter

Figure A.1 Measurements in Manual Method (a) Supra-renal angle (b) Aneurysm length of the AAA (c) Infra-renal angle (d) Proximal neck length of the AAA (e) Neck diameter

Figure A.1 shows the measurement process over MPR images in manual method. In AMET, anatomical features are measured over a 3D model. AMET provides

several modules to generate the 3D model. “DICOM Image Loader and Viewer Module” is used to explore the DICOM dataset. In Figure 6, images in the patient dataset are displayed in “DICOM Tree” panel. Physicians can navigate through the images in order to select the image where segmentation will be initialized. Selected image is displayed in “DICOM Image Editor” panel. In segmentation module, seed points are determined over this panel by using right-click menu. While seed points are selected, they are listed as reference points in “Segmentation” panel. Segmentation process is initialized from the selected image according to these reference points and determined threshold values. In “DICOM Image Editor” panel, point intensity value is displayed in the status bar by mouse-over functionality. Physicians determine the threshold upper/lower values by using this intensity values.



Figure A.2. AMET Dicom Image Loader and Viewer Module, Aortic Segmentation Module (1) DICOM Tree Panel (2) Patient Info Panel (3) DICOM Image Editor (4) Segmentation Panel

Subsequent to segmentation process, outer boundary voxels of the aorta and ACLP are produced as points in coordinate system. Generated point data is displayed in “3D view” panel reflecting the structure of the aorta. Physicians use the “Measurement Panel” to make measurements over the model (see Figure A.2). There are 3 different options; “length measurement”, “diameter measurement” and “angle measurement”. To obtain length of a desired part two reference points on the model should be selected. On the other hand, three reference points residing on the ACLP

are necessary for infra-renal and supra-renal angle measurement. Diameter of the aorta is calculated by either using “length measurement” option or “diameter measurement” option.

Anatomical features such as proximal neck length, supra-renal angle etc. are listed in “Measurement Report” panel. Each measurement value is stored in “Measurement History” panel. Physicians can drag these values to “Measurement Report” panel and map with anatomical features. A patient report is generated with mapped values.

B. Report Generation Module In AMET

Physicians are able to extract aortic feature measurements from medical using Aortic Aneurysm Measurement and Evaluation Tool. Three types of measurement classes are defined in measurement environment. These are:

- **Diameter Measurement** : Since aorta has a tubular structure, it is possible to get a diameter measurement in each region.
- **Length Measurement** : The length measurement is not defined as direct distance between two points in AMET. The length on the curved structure of the is gathered over Aortic Center Line Path. This method provides more accurate values.
- **Angle Measurement** : Since the aorta has a curved structure, there are several angulations. Angulations are also calculated via Aortic Center Line Path.

As mentioned earlier, stent device planning and sizing worksheets are used to determine the type and size of the stent graft. AMET has the capability to group and match the generated measurements with aortic features. In this way, the measurements become semantically meaningful. In Figure B.1, measurement parameters and “Measurement Report” section of AMET are depicted.

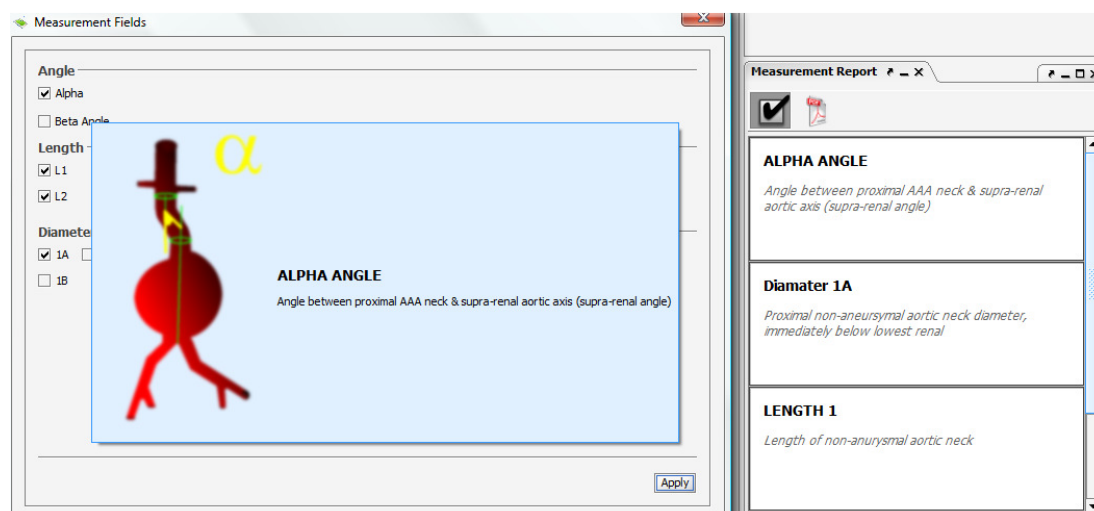


Figure B.1. Measurement Parameters and Report in AMET

This study is interested in a few aortic parameters, but developed aneurysm measurement and evaluation tool provides a detailed list of parameters. All parameters that may be obtained from abdominal aorta region are shown in Figure B.2. Iliac artery related features are also included in the list. The left part of the figure displays the whole aneurysm region with renal and iliac arteries. The right part of the figure displays the iliac region of the aorta.

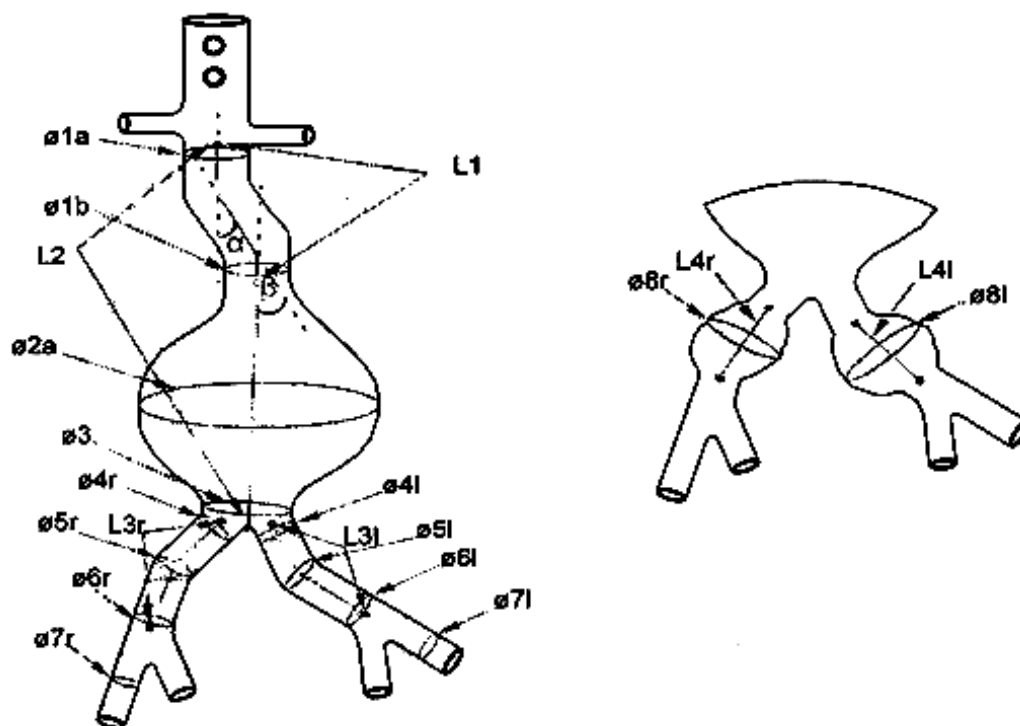


Figure B.2. Measurement parameters in abdominal aorta region.

The following table (Table B.1) lists all parameters and their brief explanation. As mentioned earlier, AMET provides three different measurement types. Each aortic feature in this list may be paired with these measurement types.

Table B.1 Measurement parameters and brief explanation

Measurement	Explanation	Unit
α Angle	Angle between proximal AAA neck & supra-renal aortic axis (supra-renal angle)	Degree

β Angle	Angle between proximal AAA neck & main axis of AAA (infra-renal angle)	Degree
Φ1a Diameter	Proximal non-aneurysmal aortic neck diameter, immediately below lowest renal	Millimeters
Φ1b Diameter	Distal non-aneurysmal aortic neck diameter, immediately above aneurysm	Millimeters
Φ2a Diameter	Maximum diameter of aneurysm	Millimeters
Φ3 Diameter	Distal diameter of aorta/aneurysm above aortic bifur	Millimeters
Φ4r Diameter	Proximal diameter of non-aneurysmal aortic neck of right iliac artery	Millimeters
Φ5r Diameter	Diameter of non-aneurysmal neck of right iliac artery	Millimeters
Φ6r Diameter	Distal diameter of non-aneurysmal neck of right iliac artery	Millimeters
Φ7r Diameter	Diameter of access vessels, right femoral artery	Millimeters

Φ4l Diameter	Proximal diameter of non-aneurysmal aortic neck of left iliac artery	Millimeters
Φ5l Diameter	Diameter of non-aneurysmal neck of left iliac artery	Millimeters
Φ6l Diameter	Distal diameter of non-aneurysmal neck of left iliac artery	Millimeters
Φ7l Diameter	Diameter of access vessels, left femoral artery	Millimeters
L1 Length	Length of non-aneurysmal aortic neck	Millimeters
L2 Length	Length from lowest renal artery to aortic bifurcation	Millimeters
L3r Length	Length of portion of right iliac from bifurcation to end of seal zone	Millimeters
L3l Length	Length of portion of left iliac from bifurcation to end of seal zone	Millimeters
Φ8r Diameter	Diameter of right iliac aneurysm	Millimeters
Φ8l Diameter	Diameter of left iliac aneurysm	Millimeters
L4r Length	Length of right iliac aneurysm	Millimeters

L4l Length	Length of left illiac aneurysm	Millimeters
-------------------	--------------------------------	-------------

C. Planes of The Body

In this dissertation, planes of the human body terms are used. In this section these planes are explained. There are three planes in the body that are used to describe the position and orientation of parts of the body. These are;

1. Sagittal plane: This plane runs through the body from the head to the feet, and divides the body into left and right halves. Any plane parallel to this through the body is known as a para-sagittal plane.
2. Coronal plane: This plane runs through the body from the head to the feet, and divides the body into front and rear halves.
3. Transverse/Axial plane: This is any plane that runs left to right through the body and divides it into upper and lower sections.
4. Oblique plane: Any plane through the body that is not parallel to one of the former three.

In Figure C.1, planes of the human body are displayed.

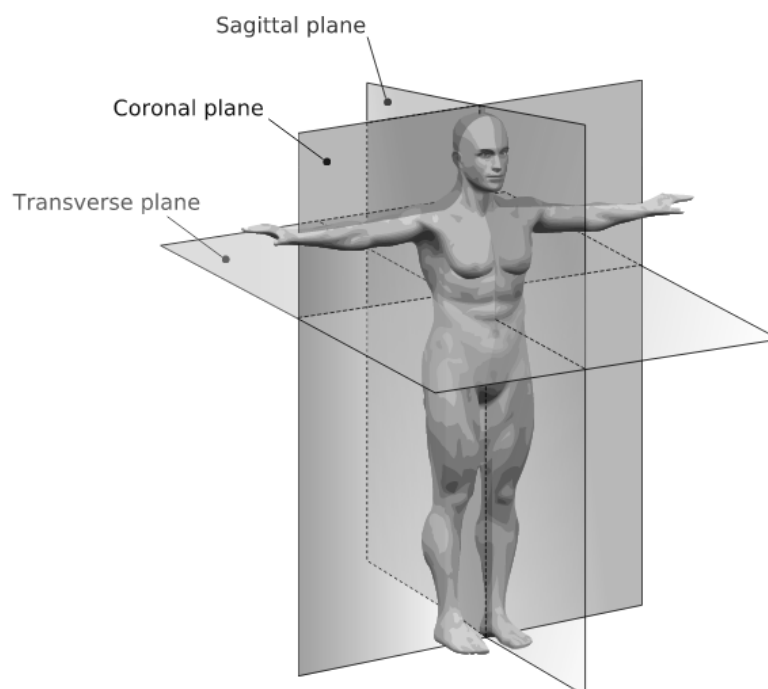


Figure C.1. Planes Of The Body

D. ABBREVIATIONS

2D	Two Dimensional
3D	Three Dimensional
AAA	Abdominal Aortic Aneurysm
ACR	American College of Radiology
AMET	Abdominal Aortic Aneurysm Measurement and Evaluation Tool
ACLP	Aortic Center Line Path
API	Application Programming Interface
BSD	Berkeley Software Distribution
CT	Computed Tomography
DICOM	Digital Imaging and Communication Standard
EVAR	Endovascular Aneurysm Repair
HTML	HyperText Markup Language
HU	Hounsfield Unit
ISO	International Organization for Standardization
ITK	Insight ToolKit
MDCT	Multi Detector Computed Tomography
MPR	Multi Planer Reformatted
MRA	Magnetic Resonance Angiography
MRI	Magnetic Resonance Imaging
NEMA	National Electrical Manufacturers Association
OpenGL	Open Graphic Library

PACS	Picture Archiving and Communication System
TCP/IP	Transmission Control Protocol/Internet Protocol
US	Ultrasonography
UV	Ultraviolet
VRML	Virtual Reality Modeling Language
XML	Extensible Markup Language